© 2020. Published by The Company of Biologists Ltd | Development (2020) 147, dev181552. doi:10.1242/dev.181552

RESEARCH ARTICLE

Laminin-binding integrins are essential for the maintenance of functional mammary secretory epithelium in lactation

Mathilde Romagnoli[1,2,*], Laura Bresson[1,2,*], Amandine Di-Cicco[1,2], María Pérez-Lanzón[1,2,‡,§], Patricia Legoix[3], Sylvain Baulande[3], Pierre de la Grange[4], Adèle De Arcangelis[5], Elisabeth Georges-Labouesse[5], Arnoud Sonnenberg[6], Marie-Ange Deugnier[1,2,7], Marina A. Glukhova[1,2,7] and Marisa M. Faraldo[1,2,7,¶]

ABSTRACT

Integrin dimers α3/β1, α6/β1 and α6/β4 are the mammary epithelial cell receptors for laminins, which are major components of the mammary basement membrane. The roles of specific basement membrane components and their integrin receptors in the regulation of functional gland development have not been analyzed in detail. To investigate the functions of laminin-binding integrins, we obtained mutant mice with mammary luminal cell-specific deficiencies of the α3 and α6 integrin chains generated using the Cre-Lox approach. During pregnancy, mutant mice displayed decreased luminal progenitor activity and retarded lobulo-alveolar development. Mammary glands appeared functional at the onset of lactation in mutant mice; however, myoepithelial cell morphology was markedly altered, suggesting cellular compensation mechanisms involving cytoskeleton reorganization. Notably, lactation was not sustained in mutant females, and the glands underwent precocious involution. Inactivation of the p53 gene rescued the growth defects but did not restore lactogenesis in mutant mice. These results suggest that the p53 pathway is involved in the control of mammary cell proliferation and survival downstream of laminin-binding integrins, and underline an essential role of cell interactions with laminin for lactogenic differentiation.

KEY WORDS: Mammary gland, Cre-Lox gene deletion, Integrin, Laminin, Differentiation, p53

INTRODUCTION

Mammary development begins during embryogenesis but the major steps of mammary morphogenesis and differentiation take place after birth (Macias and Hinck, 2012). At puberty, the mammary ducts grow and ramify. During pregnancy, the mammary epithelium undergoes a massive expansion characterized by ductal side-branching and the formation of alveoli: the milk-secreting units. During lactation, the gland achieves its fully differentiated phenotype, in response to the stimulus of suckling. Finally, when the offspring are weaned, the programmed death of most of the secretory epithelial cells results in post-lactational gland regression, also known as involution.

The cell fate decisions occurring during the various steps of postnatal mammary morphogenesis and differentiation are regulated mainly by systemic hormones and soluble growth factors (Brisken and Ataca, 2015). Moreover, cell interactions with the extracellular matrix (ECM) modulate cellular responses to the local signals provided by growth factors and hormones, thereby controlling all aspects of mammary gland development and function (Glukhova and Streuli, 2013; Muschler and Streuli, 2010).

The mammary epithelium comprises two layers: a layer of luminal cells, which produce milk during lactation; and a layer of basal myoepithelial cells, with contractile properties responsible for the expulsion of milk from the gland. The basal cells express the basal-specific keratins K5 and K14, smooth-muscle contractile proteins, such as α-smooth muscle actin, and the transcription factors p63 and Slug. The luminal cells express K8 and K18 keratins, and include a population of cells expressing the receptors for estrogen and progesterone (ER and PR, respectively). These ER/PR$^+$ cells act as hormone sensors through the production of diverse paracrine signals controlling basal and luminal cell function (Brisken and Ataca, 2015).

The remarkable regenerative properties of the mammary epithelium, reflected in the replenishment of the gland in successive pregnancies, are ensured by the presence of mammary stem cells in adult tissue (Visvader and Smith, 2011). Functional studies with sorted mammary cells have revealed that the basal compartment contains multipotent stem cells from which a functional gland can be regenerated upon transplantation, whereas the luminal cell layer contains clonogenic cells: the luminal progenitors (Asselin-Labat et al., 2007; Blaas et al., 2016; Shackleton et al., 2006; Sleeman et al., 2007; Stingl et al., 2006). This population, comprising ER/PR$^+$ and ER/PR$^-$ progenitor cells, ensures the expansion of the luminal compartment within the ducts (at puberty) and the alveoli (during pregnancy), as recently shown by lineage-tracing studies (Blaas et al., 2016; Elias et al., 2017; Rios et al., 2014; Rodilla et al., 2015; Van Keymeulen et al., 2017, 2011; Wang et al., 2017). Attention has recently focused on the ER/PR$^-$ luminal progenitors, which are thought to give rise to basal-like BRCA1-associated breast tumors in humans and mice (Lim et al., 2009; Molyneux et al., 2010).

Integrins, the major cellular ECM receptors, act as membrane sensors connecting the matrix to the cytoskeleton, and triggering the biochemical and mechanical signals that control cell phenotype and fate decisions (Glukhova and Streuli, 2013). Integrins are heterodimers consisting of an α and a β subunit. Twenty-four integrin dimers with different substrate specificities have been described (Barczyk et al., 2010; Hynes, 2002). In the mammary

[1]Institut Curie, PSL Research University, CNRS, UMR144, F-75005 Paris, France. [2]Sorbonne Universités, UPMC Univ Paris 06, F-75005 Paris, France. [3]Institut Curie Genomics of Excellence (ICGex) Platform, Institut Curie, 75005 Paris, France. [4]GenoSplice Technology, F-75005 Paris, France. [5]Institut de Génétique et de Biologie Moléculaire et Cellulaire, CNRS UMR7104/INSERM U964/ULP, F-67404 Illkirch, France. [6]Division of Cell Biology, The Netherlands Cancer Institute, 1066 CX Amsterdam, The Netherlands. [7]Inserm, Paris, F-75013 Paris, France.
*Present address: Institut de Recherche Servier, F-78290 Croissy, France. ‡Present address: Centre de Recherche des Cordeliers, INSERM, F-75006 Paris, France. §Present address: Faculty of Medicine, Paris Sud/Paris XI University, 94270 Le Kremlin-Bicêtre, France.

¶Author for correspondence (maria-luisa.martin-faraldo@curie.fr)

M.M.F., 0000-0001-9497-1171

Received 17 June 2019; Accepted 16 January 2020

Development (2020) 147, dev181552. doi:10.1242/dev.181552

gland, the basal cells are continuously exposed to the ECM, whereas the luminal cells form contacts with the basement membrane, particularly in the alveoli during pregnancy and lactation. Nevertheless, integrins are present in basal and luminal cells throughout the gland and at all developmental stages. Several genetic studies, including some by our group, have shown that β1 integrins play an important role in controlling proliferation, survival and lactational differentiation in the mammary gland (Faraldo et al., 1998, 2002; Li et al., 2005; Naylor et al., 2005). Deletion of the β1 integrin subunit gene from basal or luminal cells compromises the regenerative potential of the mammary epithelium, suggesting a role for β1 integrins in the maintenance of the stem cell pool (Li et al., 2005; Taddei et al., 2008). The β1 integrin chain can bind different α subunits, which determine the ECM ligand specificity of the resulting dimer. Little is known about the contribution of individual integrin dimers to mammary gland development.

Like several other epithelia, the mammary bilayer sits on a specialized ECM, the basement membrane, which has laminins (LNs) as one of its major components. Pioneering studies have shown that LNs are required for the induction of lactogenic differentiation by prolactin in cultured mammary cells (Streuli et al., 1995). Several LN-binding integrin dimers – α3β1, α6β1 and α6β4 – are present in the mammary epithelium during development (Raymond et al., 2012). Here, we have studied the role of these integrins in mammary development using a Cre-Lox approach in which the *Itga3* and/or *Itga6* genes were deleted *in vivo* from the luminal ER/PR^{-} progenitor cells. We found that LN-binding integrins contributed to the regulation of luminal progenitor activity and alveologenesis during pregnancy. Moreover, in the absence of these integrins, changes in cell polarity and unscheduled involution prevented sustained lactation. Importantly, the deletion of p53 rescued the growth defects observed in the absence of LN-binding integrins, but was not sufficient for the re-establishment of correct lactogenesis, suggesting these integrins play an essential role in mammary gland differentiation.

RESULTS

The deletion of LN-binding integrins affects mammary alveologenesis and luminal progenitor function in pregnancy

We first assessed the expression of integrin subunits in luminal mammary cells from virgin mice by FACS analysis (Fig. S1). The two luminal populations – progenitors (mostly ER^{-}) and mature (ER^{+}) cells – were separated on the basis of their ICAM1 expression, as previously described (Chiche et al., 2019; Di-Cicco et al., 2015; Fig. S1A). Both luminal populations were found to express several integrin receptors on their surface, including those for laminins, collagens and fibronectin (Fig. S1B). Consistent with previous findings, luminal progenitors (ICAM1^{+} population) expressed higher levels of α2 and β3 integrins than mature luminal cells (ICAM1^{-} population) (Asselin-Labat et al., 2007; Shehata et al., 2012). They also strongly expressed α3, α6, β1 and β4 integrins: the subunits of the major laminin receptors (α3β1, α6β1 and α6β4; Fig. S1B).

To study the role of LN-binding integrins in mammary lobulo-alveolar development and lactogenic differentiation, *BlgCre* mice were crossed with mice carrying conditional alleles of the *Itga3* and *Itga6* genes (*itga3*$^{F/F}$ and *itga6*$^{F/F}$). The Rosa26*LacZ*-reporter allele (R26R$^{F/+}$) was used to monitor integrin deletion. The *Blg* promoter is active in luminal cells, from mid-pregnancy onwards (Naylor et al., 2005; Selbert et al., 1998). Consistently, immunofluorescence analysis of *BlgCre;Itga3*$^{F/F}$*;Itga6*$^{F/F}$ females (referred to hereafter as α3α6KO) at 15 days of pregnancy showed a depletion of α3 and α6 integrins from most of the alveolar luminal cells (Fig. 1A). This integrin depletion in luminal cells was also confirmed by FACS and RT-qPCR analyses of mammary cells isolated from 15-day-pregnant mice (Fig. 1B, Fig. S2A,B). A previous study showed that the *Blg* promoter specifically targeted the ER/PR^{-} luminal progenitor population (Molyneux et al., 2010). Accordingly, immunofluorescence labeling revealed that the rare cells retaining α6 integrin expression in pregnant α3α6KO mouse mammary glands also expressed PR, and therefore belonged to the ER/PR^{+} lineage (Fig. 1C).

We then performed immunofluorescence and FACS analyses to determine whether the loss of the α3 and α6 chains affected the expression of other integrins. Notably, surface expression of the β1 and β4 integrins was severely impaired in the luminal cells of α3α6KO females (Fig. 1A,D). The expression of other integrins was not significantly affected in luminal cells lacking LN-binding integrins (Fig. S2B,C).

Histological analysis of the mammary glands from 15-day-pregnant mice revealed an underdevelopment of the lobuloalveolar tissues in α3α6KO females, with alveolar structures that were smaller and less numerous than in control females (Fig. 1E). In agreement with the integrin expression data, X-gal staining showed that the majority of the luminal cells were LacZ^{+}, indicating that Cre-mediated recombination had occurred in α3α6KO females (Fig. S2D). We investigated whether the observed phenotype was a consequence of impaired luminal progenitor cell activity, by performing 3D mammosphere assays with sorted luminal cells from mice at 15 days of pregnancy, as previously described (Chiche et al., 2013). Notably, the clonogenic activity of integrin-depleted luminal cells was half that in wild-type cells, whereas that of basal cells was unaffected (Fig. 1F, Fig. S2E). The mammary growth defects displayed by α3α6KO females persisted until the end of pregnancy, as shown by whole mount carmine staining of mammary glands from 18-day-pregnant females and clonogenicity assays performed with sorted luminal cells (Fig. S2F,G).

Consistent with an alveolar maturation defect, RT-qPCR analyses of milk protein genes revealed significantly lower levels of *Wap*, *Lalba* and *Csn2* (encoding whey acidic protein, α-lactalbumin and β-casein, respectively) expression in α3α6KO luminal cells from 15-day- and 18-day-pregnant females (Fig. 1G, Fig. S2H). We performed mammary organoid culture to analyze the response of the mammary epithelium to prolactin: the major regulator of lactogenic differentiation. The addition of prolactin to control explants induced the accumulation of lipid droplets in the cell cytoplasm and a 2000-fold increase in β-casein expression, as assessed by RT-qPCR (Fig. S3A). By contrast, cytoplasmic lipid droplets were rarely seen in α3α6KO organoids, and the induction of β-casein in response to prolactin was severely impaired (Fig. S3A). We also used mammary organoids to analyze branching morphogenesis, which precedes alveologenesis during pregnancy. As previously described for organoids isolated from virgin females, bFGF induced growth and branching in wild-type organoids from mice at 15 days of pregnancy (Ewald et al., 2008; Fig. S3B). By contrast, α3α6KO organoids were completely unable to branch in response to bFGF (Fig. S3B).

We performed comparative global gene expression analyses on control and α3α6KO luminal cells with Affymetrix arrays. The expression of *Muc1* and *Tjp1* (encoding the tight junction protein ZO-1), which is involved in the establishment of baso-apical polarity in the mammary epithelium, was altered in mutant cells (Fig. 1H). In addition, Reactome pathway analysis indicated lower levels of expression for circadian genes and an activation of the

Development (2020) 147, dev181552. doi:10.1242/dev.181552

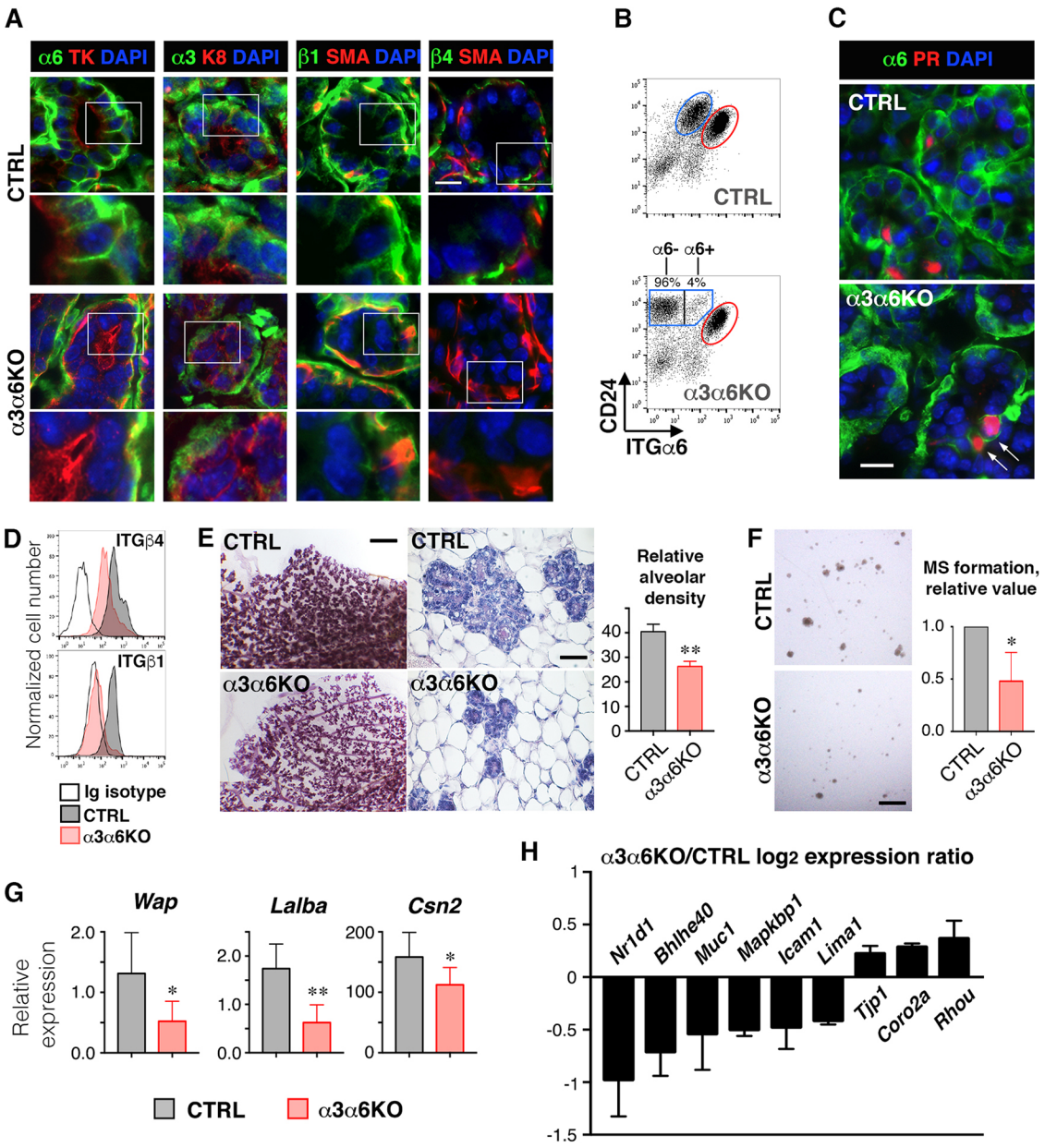

Fig. 1. Lack of laminin binding integrins affects mammary alveologenesis and luminal progenitor function in pregnancy. (A) Immunofluorescence labeling of sections through 15-day-pregnant mammary gland with antibodies against α3, α6, β1 and β4 integrins (green), pankeratin (TK), keratin 8 (K8) and α-smooth-muscle actin (SMA) (red). The α3 and α6 staining encircling the alveoli reflects untargeted basal cell displaying normal integrin expression. DAPI serves to visualize nuclei. Areas within rectangles are shown at 2.5× higher magnification below each image. Scale bar: 10 µm. (B) Dot plots showing separation of luminal (blue oval) and basal (red oval) epithelial cells from 15-day-pregnant mouse mammary glands by flow cytometry. A representative experiment is shown. Most of the luminal cells from α3α6KO mice are negative for α6 integrin. (C) Immunofluorescence labeling of sections through 15-day-pregnant mouse mammary gland with antibodies against α6 integrin and progesterone receptor. DAPI served to visualize nuclei. Arrows show cells co-expressing α6 integrin and PR in the α3α6KO gland. Scale bar: 10 µm. (D) Histograms showing expression of β1 and β4 integrins in luminal cells from 15-day-pregnant mammary glands. (E) Microphotographs of 15-day-pregnant control and α3α6KO mouse mammary glands. Left: fragments of glands stained with Carmine in whole-mount. Scale bar: 0.8 mm. Right, Hematoxylin and Eosin staining of gland sections. Scale bar: 40 µm. The graph shows quantification of the relative alveolar density (mean±s.d.) obtained from three animals per genotype. P=0.004. (F) Mammosphere formation by luminal cells sorted from 15-day-pregnant mouse mammary glands. Left: representative microphotographs. Scale bar: 750 µm. The graph shows quantification of mammosphere number (mean±s.d.) obtained from four independent experiments. P=0.03. Values obtained for control cells were set as 1 in each experiment. (G) RT-qPCR analysis of milk protein gene expression in freshly sorted luminal cells from 15-day-pregnant mouse mammary glands. The values shown are mean±s.d. obtained from four independent experiments. P=0.03 for *Wap*, 0.003 for *Lalba* and 0.027 for *Csn2*. (H) RT-qPCR analysis of gene expression in freshly sorted luminal cells from 15-day-pregnant mouse mammary glands. The values shown are mean±s.d. obtained from three independent experiments. P<0.05 for all genes analyzed.

Rho/formins pathway in α3α6KO cells (Table S1). Other genes differentially regulated in control and mutant cells included *Lima1* and *Coro2a*, encoding proteins involved in actin regulation. Furthermore, we observed changes in the expression levels of several genes (*Mapkbp1*, *Icam1* and *Zc3h12c*) connected to the NF-κB signaling pathway, an important regulator of mammary alveologenesis (Fernandez-Valdivia et al., 2009). The differential expression of several genes was confirmed by RT-qPCR (Fig. 1H).

Development (2020) 147, dev181552. doi:10.1242/dev.181552

Altogether, these results indicate that the depletion of LN-binding integrins affects the function of mammary luminal progenitors, perturbs mammary development and impairs lactogenic differentiation during pregnancy.

The deletion of LN-binding integrins affects luminal progenitor activation in response to ovarian hormones

The ovarian hormones estrogen (E) and progesterone (P) play an important role in inducing the paracrine signals contributing to the changes occurring in the mammary gland during early pregnancy (Brisken and O'Malley, 2010). We therefore compared the responses of control and mutant epithelia to ovarian hormone treatment mimicking early events in pregnancy. The E/P stimulation of control virgin females induced intense ductal side branching accompanied by alveolus formation in the mammary glands (Fig. 2A, upper panels). By contrast, in α3α6KO glands, side branching was impaired and alveolar density was only half that in the control glands (Fig. 2A, lower panels). Consistently, proliferation was impaired in α3α6KO epithelium, as assessed by Ki67 immunolabeling (Fig. 2B). FACS analysis of E/P-stimulated glands revealed the presence of a population of luminal cells devoid of α6 integrin in mutant mouse glands, confirming Blg promoter-driven Cre induction (Fig. 2C). RT-qPCR confirmed the deletion of *Itga3* and *Itga6* in α3α6KO luminal cells (Fig. S4A). As expected, integrin depletion occurred essentially in the ICAM1$^+$ luminal progenitor population, in which more than 70% of the cells were devoid of α6 integrin (Fig. 2D).

To study the individual contribution of α3 and α6 integrins in the observed phenotype, we analyzed the effect of ovarian hormone

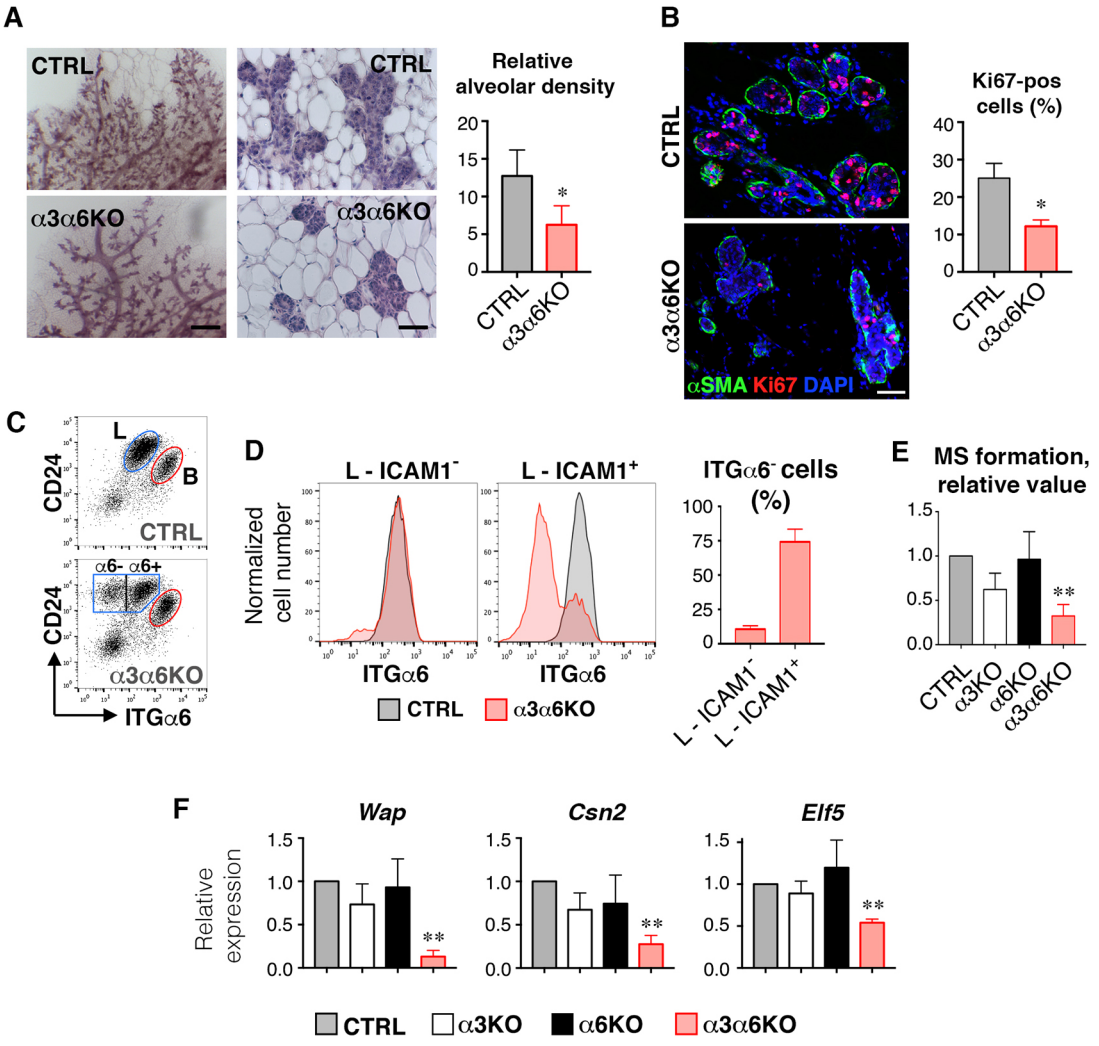

Fig. 2. The deletion of LN-binding integrins affects luminal progenitor activation in response to ovarian hormones. (A) Microphotographs of E/P-stimulated control and α3α6KO mouse mammary glands. Left: fragments of glands stained with Carmine in whole mount. Scale bar: 400 µm. Right, Hematoxylin and Eosin staining of gland sections. Scale bars: 40 µm. The graph shows quantification of the relative alveolar density (mean±s.d.) obtained from four independent experiments. *P*=0.026. (B) Immunofluorescence staining of control and α3α6KO mouse mammary gland sections with antibodies against Ki67 and αSMA. Scale bar: 40 µm. The graph shows quantification of Ki67-positive cells (mean±s.d.) obtained from three animals per group. *P*=0.017. (C) Dot plot showing separation of luminal (L) and basal (B) epithelial cells from E/P-stimulated mammary glands by flow cytometry. In α3α6KO mice, a fraction of the luminal cell population is devoid of α6 integrin expression. (D) Histograms showing expression of α6 integrin in mature luminal cells (L-ICAM1$^-$) and luminal progenitors (L-ICAM1$^+$) from E/P-stimulated mammary glands by flow cytometry. L-ICAM1$^-$ and L-ICAM1$^+$ populations were separated as described in Fig. S1A. The graph shows the percentage of α6 integrin-negative luminal cells in both luminal populations (mean±s.d.) obtained from five independent experiments. (E) Mammosphere formation capacity of luminal progenitor cells isolated from E/P-stimulated mammary glands. Data are mean±s.d.; *n*=3 (α3KO and α6KO) or *n*=5 (Ctrl and α3α6KO) independent experiments; *P*=0.0003. (F) RT-qPCR analysis of gene expression in freshly sorted luminal progenitor cells from E/P-stimulated mammary glands. Data are mean±s.d. obtained from three independent experiments. *P*=0.007 for *Wap*, 0.003 for *Csn2* and 0.009 for *Elf5*.

Development (2020) 147, dev181552. doi:10.1242/dev.181552

induction in Blgcre;*itga3*$^{F/F}$ and Blgcre;*itga6*$^{F/F}$ mice (referred to hereafter as α3KO and α6KO, respectively). The morphology of the α3KO and α6KO mammary glands after E/P stimulation was similar to that of the mammary glands of stimulated control littermates (Fig. S4B). Furthermore, luminal ICAM1^{+} progenitors were isolated from control, α3KO, α6KO and α3α6KO mammary glands, as shown in Fig. S4C, and their clonogenic potential was analyzed in mammosphere assays. We found that simultaneous deletion of the α3 and α6 genes, but not of either of these genes separately, significantly decreased the clonogenic capacity of luminal progenitors (Fig. 2E). In addition, expression of the milk protein genes *Wap* and *Csn2* was very weak in α3α6KO luminal progenitors, but not significantly affected in α3KO and α6KO cells (Fig. 2F). Finally, in α3α6KO luminal cells, the expression of *Elf5*, encoding a transcription factor essential for alveologenesis, was half that in control cells (Fig. 2F).

We have previously reported that, from mid pregnancy, the luminal mammary population is particularly enriched in Sca-1^{-}/ICAM1^{+} cells potentially representing alveolar progenitors (Chiche et al., 2019; Di-Cicco et al., 2015). Consistently, we found that this luminal subpopulation (referred to hereafter as Lu4) was decreased in α3α6KO glands, and displayed poor clonogenicity and low levels of milk protein gene expression (Fig. S4D-F). Notably, an efficient depletion of α3 and α6 integrins was detected in the Lu4 subpopulation, indicating that the Blg promoter is specifically active in these cells (Fig. S4F).

Altogether, our results indicate that the α3 and α6 integrins are implicated in the response of mammary epithelial cells to ovarian hormone stimulation, including luminal progenitor cell proliferation and differentiation into milk-secreting cells.

The deletion of LN-binding integrins leads to basal cell shape changes but does not affect early lactation

We then analyzed the impact of LN-binding integrin gene deletion on lactation. On the second day of lactation, the mammary glands of α3α6KO females displayed lobuloalveolar development similar to that of the control glands, with dense secretory tissue and almost no fat pad stroma (Fig. 3A). Levels of milk protein gene transcripts in the luminal cells of α3α6KO mice were not significantly different from those in control mice, indicating that the alveoli were functional (Fig. 3B). Consistently, the weights of pups fed by control and mutant females were similar on day 2 of lactation (Fig. 3C). However, the level of phosphorylation of FAK, an important downstream effector of integrins, was lower in α3α6KO glands (Fig. S5A).

The depletion of LN-binding integrins was confirmed by FACS or RT-qPCR (Fig. S5B,C). Morphological analyses of the

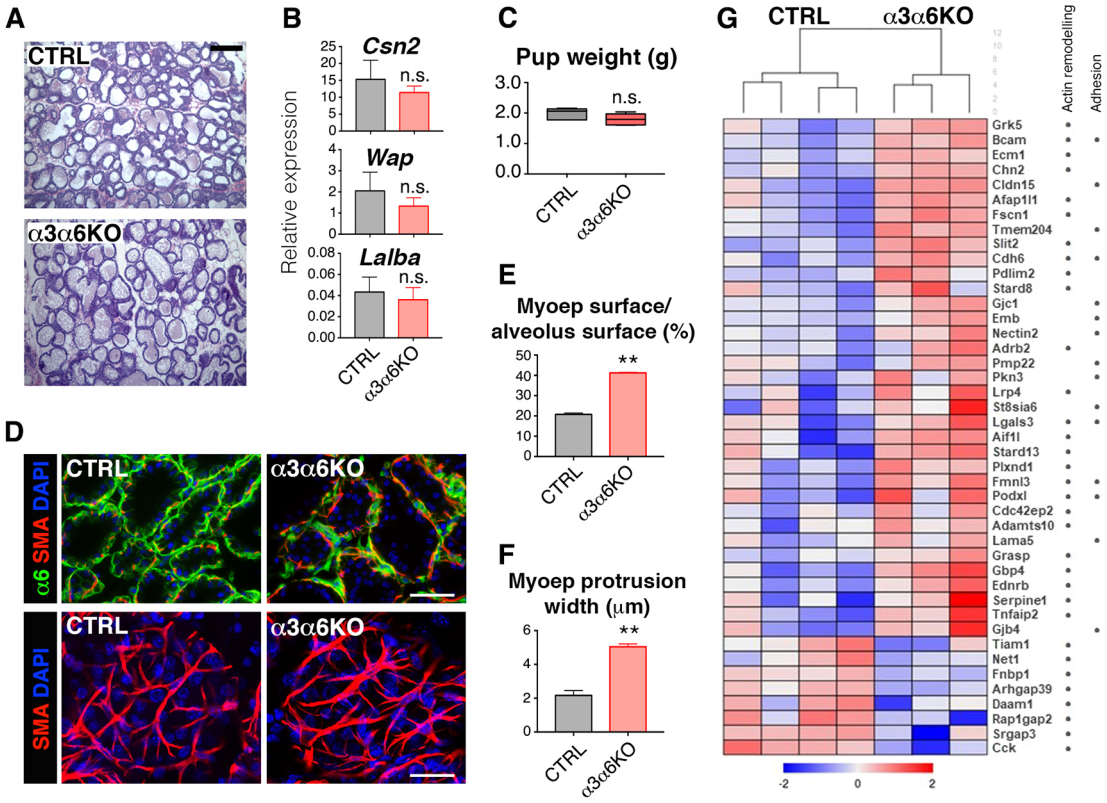

Fig. 3. The deletion of LN-binding integrins leads to basal cell shape changes but does not affect early lactation. (A) Hematoxylin and Eosin staining of sections through 2-day-lactating mammary glands of control and α3α6KO females. Scale bar: 150 µm. (B) RT-qPCR analysis of milk protein gene expression in freshly isolated luminal cells sorted from 2-day-lactating mammary glands. Data are mean±s.d. obtained from four independent experiments; n.s., not statistically significant. (C) Weight of the pups fed by control or α3α6KO females for 2 days. The litters from six females per genotype were analyzed; the boxes represent the interquartile range, the line in the box is the median and the whiskers indicate the minimum and maximum values; n.s., not statistically significant. (D) Immunofluorescence labeling of sections through 2-day-lactating mouse mammary glands with antibodies against α6 integrin and α-smooth-muscle actin (SMA). DAPI served to visualize nuclei. Confocal images are shown. Scale bars: 62 µm (upper panels); 25 µm (lower panels). (E) The percentage of the alveolar surface covered by basal SMA^{+} cells. Data are mean±s.d. obtained from three control and three α3α6KO mammary glands at 2 days of lactation; at least eight alveoli were quantified for each animal. *P*=0.0001. (F) Branch cell width of alveolar basal cells. Data are mean±s.d. obtained from three control and three α3α6KO mammary glands at 2 days of lactation; at least 20 cells were quantified for each animal. *P*=0.0004. (G) Heatmap based on RNA-seq analysis showing genes differentially expressed in freshly isolated control and α3α6KO mammary basal cells from 2-day-lactating mice. Four control and three α3α6KO females were analyzed.

Development (2020) 147, dev181552. doi:10.1242/dev.181552

mammary glands in early lactation were performed using double immunofluorescence labeling of tissue sections. Consistent with FACS analysis, the luminal cells of mutant glands were devoid of α6 integrin, whereas this integrin was detected in the basal cells (Fig. 3D, Fig. S5B). In sections through control glands, basal myoepithelial cells, detected by α-smooth muscle (αSMA) labeling, appeared as rare spots decorating the basal side of the alveoli. By contrast, the myoepithelial cells in integrin-depleted glands formed a more continuous layer around luminal cells (Fig. 3D, upper panels). Confocal microscopy revealed that myoepithelial cell shape was profoundly altered in the mammary alveoli of α3α6KO females (Fig. 3D, lower panels). In particular, the myoepithelial cells in the mutant epithelium had thicker protrusions and covered a larger area of the alveoli than the myoepithelial cells of control glands (Fig. 3D-F). To investigate the molecular alterations accounting for these morphological changes, we performed RNA-seq analysis on freshly sorted basal cells from control and α3α6KO mice. Several genes (including *Nectin2*, *Gjc1*, *Cldn15*, *Emb* and *Lama5*), encoding proteins involved in cell-cell or cell-substrate adhesion were more strongly expressed in mutant females than in controls (Fig. 3G). In addition, we observed changes in the expression of numerous genes involved in the regulation of actin dynamics and cell shape (Fig. 3G). These results reveal that, at the beginning of lactation, the mammary alveoli of mutant females present major alterations in basal cell morphology, despite being apparently functional.

LN-binding integrin depletion disturbs luminal cell baso-apical polarization and leads to unscheduled involution

We investigated whether lactation could proceed normally beyond day 2 in the absence of LN-binding integrins, by comparing the mammary phenotypes of control and mutant females at the time of pup weaning on day 21. The glands from α3α6KO females presented collapsed, dispersed alveolar structures reminiscent of those found in involuting tissues, a morphology different from that of control tissue (Fig. 4A, Fig. S6A). The glands of α3KO females were similar to those of control animals, whereas α6KO females displayed slightly less developed glands (Fig. 4A). Pups fed by α3α6KO females were significantly lighter than pups fed by control mice, from day 14 of lactation (Fig. 4B). Consistently, the level of expression of milk protein genes was significantly lower in α3α6KO glands (Fig. 4C). The pups fed by α3KO females were of normal weight, whereas those fed by α6KO females were significantly lighter after 21 days of lactation (Fig. 4B). At this stage, the expression of milk protein genes was impaired in α6KO glands (Fig. S6B).

A more detailed histological analysis of glands at 14 days of lactation revealed that, unlike the flat luminal cells typically observed in control alveoli full of milk, the luminal cells in α3α6KO tissue were frequently protruding into the lumen (Fig. 4D, Fig. S6C). Using immunofluorescence labeling, we analyzed the distribution of polarity markers in α3α6KO epithelium. The *cis*-Golgi marker protein GM130, which was located in an apical position facing the lumen in control luminal cells, was abnormally distributed in about 12% of luminal cells of α3α6KO alveoli (Fig. 4E,F). Two types of abnormal Golgi localization were observed: cells in which GM130 labeling revealed a normal ribbon-like Golgi with aberrant basal localization (Fig. 4E, central picture); and cells with a dispersed Golgi, also basally located with respect to the nucleus (Fig. 4E, right picture). In these abnormal mutant cells, the polarity marker Par3, normally presenting an apico-lateral distribution in control epithelium, was either absent or basally located, indicating a disruption of polarity (Fig. 4F). In addition, E-cadherin was often found at the apical side of luminal α3α6KO cells with aberrant morphology (Fig. 4G). Although immunolabeling for laminin did not reveal major perturbations in basement membrane integrity (Fig. 4G), expression of *Lamb3*, a gene coding for the β3 chain, a component of laminin 332 (laminin 5), one of the major constituents of the mammary basement membrane, was increased in α3α6KO glands (Fig. S6D). Finally, FAK phosphorylation levels were lower in α3α6KO glands at lactation day 14, confirming a perturbation of luminal cell interactions with ECM (Fig. S6E).

The secretory tissue hypoplasia observed in α3α6KO glands suggested that precocious cell death might be associated with LN-binding integrin deletion. To analyze apoptosis rates in mammary tissues lacking LN-binding integrins, we performed TUNEL assays with sections through day 21 lactating glands; the number of TUNEL-positive cells was greater in α3α6KO females (Fig. 4H). Increases in cathepsin D expression and lysosomal release during involution-associated cell death have recently been reported (Sargeant et al., 2014). Consistently, cells expressing cathepsin D were detected in the mutant tissue (Fig. S6F). Finally, the expression of *Lif* (encoding leukemia inhibitory factor), an essential factor for the regulation of cell death during mammary involution, was strongly increased during late lactation in α3α6KO tissues (Kritikou et al., 2003; Schere-Levy et al., 2003; Fig. 4I). Together, these results show that the depletion of LN-binding integrins in luminal cells perturbs baso-apical polarization and induces early cell death and unscheduled secretory tissue involution, preventing full lactation.

Genetic p53 suppression restores growth but not differentiation in mammary luminal cells depleted of LN-binding integrins

We recently showed that, in the absence of LN-binding integrins, the clonogenic activity of basal mammary cells was inhibited by a mechanism involving p53 activation (Romagnoli et al., 2019). Analysis of the microarray data obtained with 15-day-pregnant mouse glands suggested an activation of the p53 pathway in α3α6KO luminal cells (Fig. 5A). Consistently, in the mammospheres generated by these cells, the expression of *Cdkn1a* (encoding the cell cycle inhibitor p21) and *Mdm2*, two important p53 targets, was increased, as assessed by qPCR analysis (Fig. 5B). To study the possible involvement of p53 deregulation in the abnormal mammary phenotype of α3α6KO mice, we crossed these mice with mice carrying conditional alleles of the *Trp53* gene ($Trp53^{Flox}$) to obtain Blgcre;$itga3^{F/F}$;$itga6^{F/F}$;$Trp53^{F/F}$ mice (referred to hereafter as α3α6p53KO). Following stimulation with ovarian hormones, the mammary glands of α3α6p53KO females presented normal side branching and an alveolar density similar to that found in control littermates (Fig. 5C). The mammospheres formed by α3α6p53KO cells did not express α6 integrin, confirming target gene deletion (Fig. 5D). Quantitative analysis revealed that the clonogenic activity of α3α6p53KO luminal progenitors was unaffected and similar to that in the controls in 1st- and 2nd-generation mammosphere assays (Fig. 5D, Fig. S7A). Nevertheless, milk protein gene expression levels were significantly lower in the α3α6p53KO luminal progenitors, indicating differentiation defects (Fig. 5E). Consistently, in mammary organoids derived from 15-day-pregnant α3α6p53KO glands, the expression of *Csn2* after prolactin induction was decreased when compared with control organoids (Fig. S7B). When treated with bFGF, α3α6p53KO organoids displayed active growth, but failed branching (Fig. S7C).

Development (2020) 147, dev181552. doi:10.1242/dev.181552

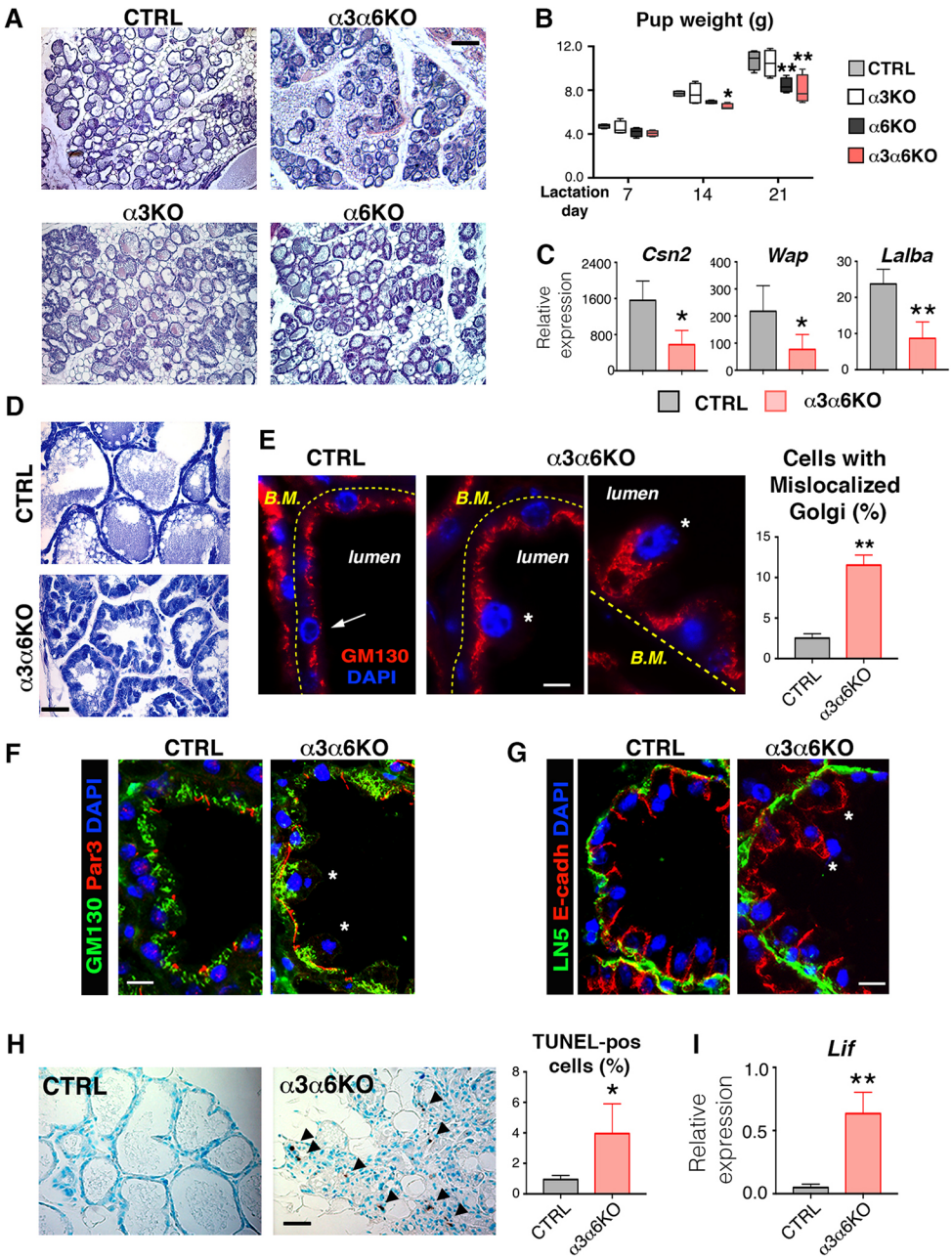

Fig. 4. The deletion of LN-binding integrins disturbs luminal cell baso-apical polarization and leads to unscheduled involution. (A) Hematoxylin and Eosin staining of sections through 21-day-lactating mouse mammary glands from control, α3KO, α6KO and α3α6KO females. Scale bar: 150 µm. (B) Weight of the pups fed by control, α3KO, α6KO or α3α6KO females after 7, 14 and 21 days of lactation. The litters from four females per genotype were analyzed; the boxes represent the interquartile range, the line in the box is the median and the whiskers indicate the minimum and maximum values; *P*=0.04 (lactation day 14) and 0.006 (lactation day 21) for α3α6KO litters, and 0.003 (lactation day 21) for α6KO litters. (C) RT-qPCR analysis of milk protein gene expression in 21-day-lactating mouse mammary glands. Data are mean±s.d.; four females per genotype were analyzed; *P*=0.012 for *Csn2*, 0.05 for *Wap* and 0.003 for *Lalba*. (D) Hematoxylin and Eosin staining of sections through 14-day-lactating mouse mammary glands. Scale bar: 30 µm. (E) Immunofluorescence labeling of sections through 14-day-lactating mouse mammary gland with an antibody against GM130. DAPI served to visualize nuclei. The basement membrane is indicated by a dotted line. The arrow shows a cell with normal apical localization of GM130; asterisks mark cells with aberrant basal GM130 localization. Scale bar: 10 µm. Data are mean±s.d., three females per genotype were analyzed and a minimum of 250 cells per sample were counted; *P*=0.002. (F,G) Immunofluorescence labeling of sections through 14-day-lactating mouse mammary gland with an antibody against GM130 and Par3 (F), and antibodies against laminin 5 and E-cadherin (G). DAPI served to visualize nuclei. Asterisks mark cells with aberrant Par3 and E-cadherin localization. Scale bar: 15 µm. (H) TUNEL assay performed with sections through 21-day-lactating mammary glands from control and α3α6KO females. Methyl Green was used as counterstaining. Arrowheads indicate TUNEL-positive cells. Scale bar: 50 µm. Data are mean±s.d., four females per genotype were analyzed, *P*=0.05. (I) RT-qPCR analysis of *Lif* expression in 21-day-lactating mouse mammary glands. Data are mean±s.d., four females per genotype were analyzed, *P*=0.005.

We further analyzed α3α6p53KO mammary glands during lactation and found that, on day 14, alveolar morphology was altered with respect to control glands, with α3α6p53KO alveoli resembling those found in α3α6KO tissue (Fig. 5F). As in p53-expressing epithelium, myoepithelial cell morphology appeared altered in the α3α6p53KO lactating glands, as shown by the

Development (2020) 147, dev181552. doi:10.1242/dev.181552

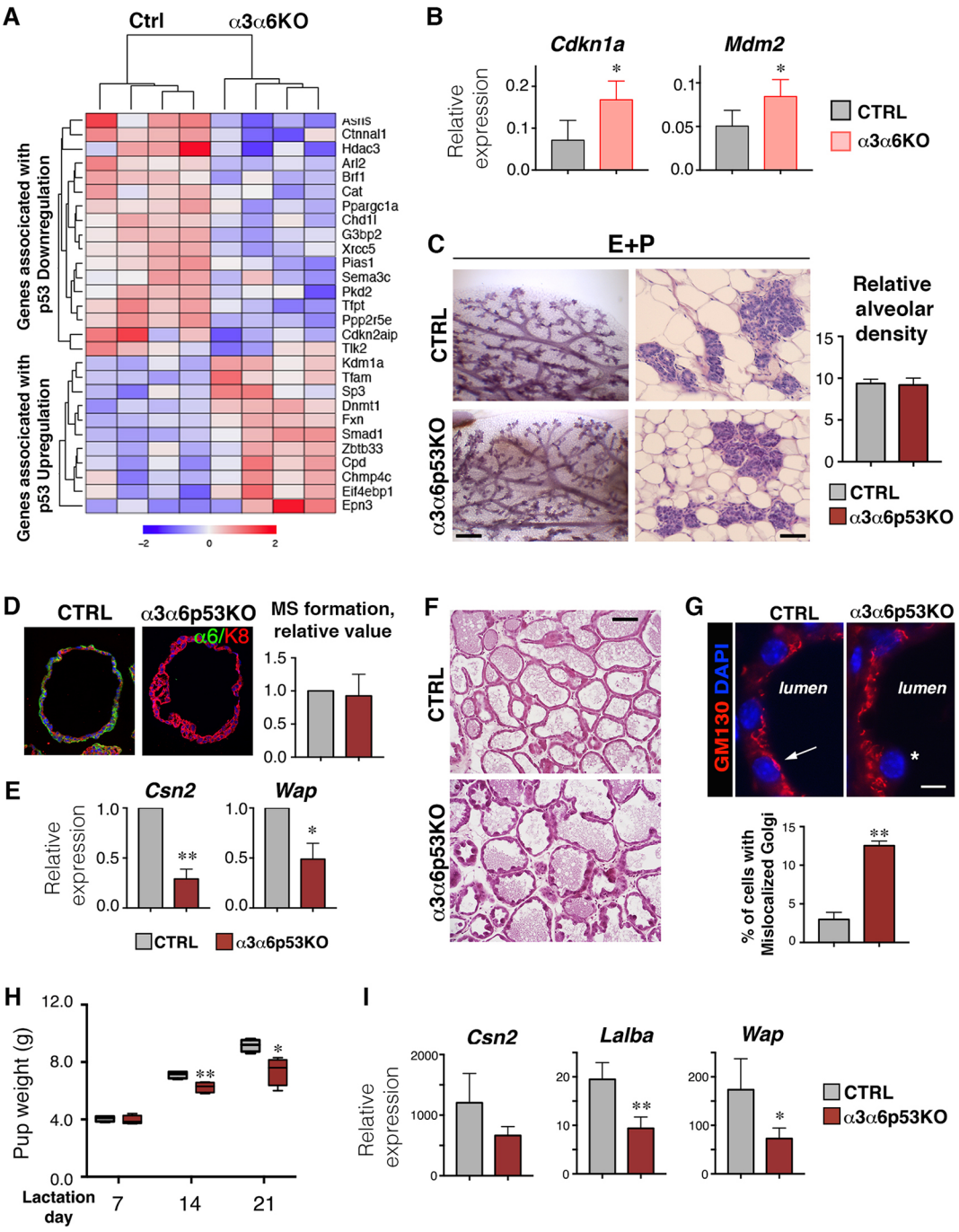

Fig. 5. Genetic p53 suppression restores growth but not differentiation in mammary luminal cells depleted of LN-binding integrins. (A) Heatmap based on microarray analysis of freshly sorted luminal progenitor cells isolated from 15-day-pregnant control and α3α6KO mammary glands. (B) RT-qPCR analysis of *Cdkn1a* and *Mdm2* gene expression in mammospheres formed by luminal progenitor cells from 15-day-pregnant control and α3α6KO mammary glands. Data are mean±s.d. obtained from four independent experiments; *P*=0.025 for *Cdkn1a* and 0.04 for *Mdm2*. (C) Photomicrographs of mammary glands from control and α3α6p53KO females stimulated with ovarian hormones (E+P). Left, whole-mount Carmine staining; right, Hematoxylin and Eosin staining. Scale bars: 400 µm (left); 40 µm (right). The graph shows quantification of the relative alveolar density (mean±s.d.) obtained from three independent experiments. (D) Immunofluorescence labeling of sections through mammospheres formed by mammary luminal progenitors sorted from E/P-stimulated control and α3α6p53KO females with antibodies against K8 and α6 integrin. Data are mean±s.d. obtained from three independent experiments. (E) RT-qPCR analysis of milk protein gene expression in freshly isolated mammary luminal progenitors sorted from E/P-stimulated control and α3α6p53KO females. Data are mean±s.d. obtained from three independent experiments. *P*=0.006 for *Csn2*, 0.03 for *Wap*. (F) Hematoxylin and Eosin staining of sections through 14-day-lactating mammary glands. Scale bar: 90 µm. (G) Immunofluorescence labeling of sections through 14-day-lactating mouse mammary gland with an antibody against GM130. DAPI served to visualize nuclei. The arrow indicates normal apical localization of GM130; asterisk indicates aberrant basal localization. Scale bar: 10 µm. Data are mean±s.d., three females per genotype were analyzed; at least 250 cells per sample were counted; *P*=0.003. (H) The weight of the pups fed by control or α3α6p53KO females after 7, 14 and 21 days of lactation. The litters (seven or eight pups) from four females per genotype were analyzed; the boxes represent the interquartile range, the line in the box is the median and the whiskers indicate the minimum and maximum values; *P*=0.008 (lactation day 14) and 0.016 (lactation day 21). (I) RT-qPCR analysis of milk protein gene expression in 21-day-lactating mammary glands from control and α3α6p53KO females. Data are mean±s.d., four females per genotype were analyzed, *P*=0.11 for *Csn2*, 0.004 for *Lalba*, 0.045 for *Wap*.

Development (2020) 147, dev181552. doi:10.1242/dev.181552

increased alveolar surface covered by basal cells (Fig. S7D). Interestingly, proliferating cells, which are rarely found in control or α3α6KO glands at 14 days of lactation, were readily detected in α3α6p53KO epithelium (Fig. S7D). In addition, as in α3α6KO p53-proficient mice, the GM130 Golgi marker Par3 and E-cadherin were frequently mislocalized, indicating alterations in epithelial cell polarity (Fig. 5G, Fig. S7E,F). The number of TUNEL-positive cells and the level of expression of *Lif* in α3α6p53KO glands on day 21 of lactation were similar to those in controls, indicating that p53 deletion interfered with the cell death caused by integrin deletion (Fig. S7G,H). However, the pups fed by α3α6p53KO mice were lighter than those fed by control mice from the middle of lactation onwards, and, consistently, the levels of expression of milk protein genes were significantly reduced (Fig. 5H,I). These results indicate that genetic inactivation of p53 rescues the growth defects, but not the impairment of epithelial polarity and lactogenic differentiation caused by the depletion of LN-binding integrins.

Activation of a Rho/myosin II/p53 pathway following depletion of LN-binding integrins in mammary luminal progenitors

We have recently reported that LN-binding integrins play an essential role in controlling the proliferative potential of mammary basal stem/progenitor cells through RhoA/ROCK/myosin II-mediated regulation of p53 (Romagnoli et al., 2019). To study whether a similar pathway operates in luminal progenitor cells, we isolated luminal ICAM^{+} cells form control, α3α6KO and α3α6p53KO virgin females, and deleted the *Itga3*, *Itga6* and *Trp53* genes *in vitro* by transduction with an adenovirus expressing Cre-recombinase (Adeno-Cre). Gene deletion was confirmed by RT-qPCR analyses (Fig. S8A). Consistent with the results obtained with freshly isolated luminal progenitors from pregnant mice, the clonogenicity of luminal progenitors was severely impaired after depletion of LN-binding integrins *in vitro* (Fig. 6A). RT-qPCR analyses performed with RNA samples obtained from dissociated mammospheres revealed an upregulation of p53 transcriptional targets such as *Cdkn1a* and *Mdm2* in α3α6KO cells, suggesting an activation of the p53 pathway in these cells (Fig. 6B, Fig. S8B). Furthermore, depletion of p53 rescued the mammosphere formation capacity of α3α6KO luminal progenitors (Fig. 6A).

Western blot analysis showed that phospho-MLC levels were increased in α3α6KO cells, indicating enhanced RhoA/ROCK activity (Fig. S8C). Consistently, analysis of the microarray data obtained from 15-day-pregnant glands suggested an enhanced Rho activity in α3α6KO luminal cells compared with control cells (Fig. S8D). Next, to study whether activation of the RhoA/ROCK/myosin II pathway could account for the impaired α3α6KO luminal progenitor activity, we performed mammosphere assays in the presence of the ROCK inhibitor Y27632 or blebbistatin, an inhibitor of myosin II activity downstream of ROCK. As shown in Fig. 6C, in

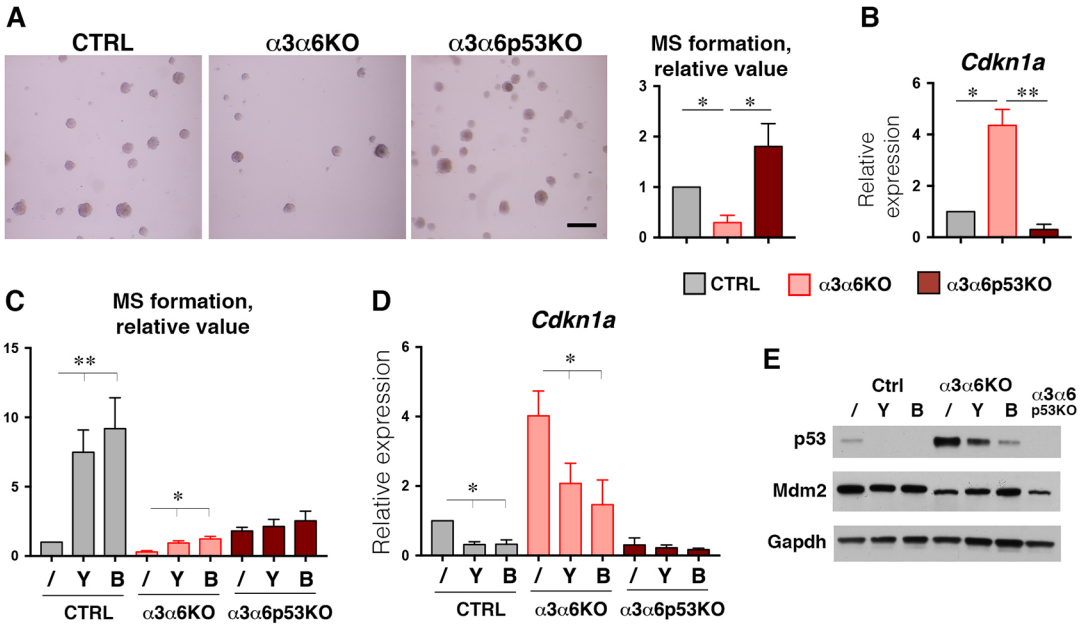

Fig. 6. Activation of a Rho/myosin II/p53 pathway following depletion of LN-binding integrins in mammary luminal progenitors. (A) Mammospheres formed by luminal progenitor cells following adenoCre-mediated integrin depletion and counted after 12 days of culture. Left: representative photomicrographs of mammospheres formed by control, α3α6KO and α3α6p53KO luminal progenitor cells. Scale bar: 400 µm. Data are mean±s.d. obtained in three independent experiments. For α3α6KO versus control, *P*=0.014; for α3α6KO versus α3α6p53KO, *P*=0.02. (B) RT-qPCR analysis of *Cdkn1a* gene expression in cells obtained from mammospheres formed by control, α3α6KO and α3α6p53KO luminal progenitor cells. Data are mean±s.d. obtained in three independent experiments. For α3α6KO versus control, *P*=0.034; for α3α6KO versus α3α6p53KO, *P*=0.001. (C) Mammosphere formation by control, α3α6KO and α3α6p53KO luminal progenitor cells in the presence of Y27632 or blebbistatin. Data are mean±s.d. obtained in three independent experiments. For control mammospheres, *P*=0.045 for Y27632-treated cells compared with non-treated cells; *P*=0.05 for blebbistatin-treated cells compared with non-treated cells. For α3α6KO mammospheres, *P*=0.033 for Y27632-treated cells compared with non-treated cells; *P*=0.024 for blebbistatin-treated cells compared with non-treated cells. (D) RT-qPCR analysis of *Cdkn1a* gene expression in cells obtained from mammospheres formed by luminal progenitor cells in the presence of Y27632 or blebbistatin. Data are mean ±s.d. obtained in three independent experiments. For control mammospheres, *P*=0.005 for Y27632-treated cells compared with non-treated cells, *P*=0.01 for blebbistatin-treated cells compared with non-treated cells. For α3α6KO mammospheres, *P*=0.006 for Y27632-treated cells compared with non-treated cells; *P*=0.023 for blebbistatin-treated cells compared with non-treated cells. (E) Western blotting analysis of p53 and MDM2 protein levels in extracts of mammosphere formed by control, α3α6KO and α3α6p53KO luminal cells. GAPDH was used as a loading control. A representative experiment is shown. Values obtained for control cells were set as 1 in each experiment. Y, Y27632; B, blebbistatin.

Development (2020) 147, dev181552. doi:10.1242/dev.181552

the presence of Y27632 or blebbistatin, the clonogenic capacity of α3α6KO cells was restored, whereas control cells presented an increase in sphere formation capacity (Fig. 6C). In contrast, these inhibitors had little effect on the clonogenicity of α3α6p53KO cells (Fig. 6C).

We next studied the effects of Y27632 and blebbistatin on p53 activity in control and integrin-depleted cells. Expression of the p53 target genes *Cdkn1a* and *Mdm2* was downregulated in the presence of the drugs, in control and mutant cells, suggesting an inhibition of p53 transcriptional activity (Fig. 6D, Fig. S8B). In line with these data, p53 protein was nearly undetectable in control cells treated with Y27632 or blebbistatin (Fig. 6E). Furthermore, the p53 protein levels were increased in α3α6KO cells. Consistently, this was accompanied by a decreased level of MDM2, a protein facilitating the p53 proteosomal degradation (Carr and Jones, 2016; Fig. 6E). Finally, inhibition of myosin II by Y27632 or blebbistatin resulted in an increase in MDM2 protein and a decrease in p53 levels in α3α6KO cells (Fig. 6E). Taken together, these data strongly indicate that the p53 pathway activation in the luminal progenitors lacking LN-binding integrins is mediated by the Rho/ROCK/myosin II axis.

DISCUSSION

This study implicates LN-binding integrins containing α3 or α6 subunits in the control of luminal progenitor expansion and alveologenesis during pregnancy, and demonstrates the requirement of these integrins for the maintenance of functional secretory tissue in lactation. Mammary basal cells are highly enriched in integrins, but luminal cells also express a panel of different integrins on their surface (Glukhova and Streuli, 2013; Raymond et al., 2012). In adult virgin mice, integrin dimers including α2 or β3 subunits, mostly functioning as receptors for collagen and fibronectin, respectively, have been used as markers for separating the luminal progenitor population from the population of ER/PR^{+} luminal cells (Asselin-Labat et al., 2007; Shehata et al., 2012). However, the role of specific integrin dimers in luminal progenitor function during mammary development has yet to be analyzed in detail.

Here, to study the roles played by LN-binding integrins in mammary luminal cells, we specifically targeted Cre expression to the luminal progenitor population with the BLG promoter, permitting deletion of α3 and/or α6 integrin chains from luminal progenitors. We found that the depletion of LN-binding integrins interfered with the expansion of luminal progenitors in pregnancy or following E/P administration. Branching morphogenesis and alveologenesis were subsequently impaired, leading to differentiation defects in the mammary epithelium of pregnant or E/P-treated mutant mice. Deletion of the p53 gene rescued hormone-induced alveolar development in α3α6KO mice, suggesting that, as previously reported for basal cells, p53 activation may contribute to the mammary growth defects observed in luminal cells depleted of LN-binding integrins (Romagnoli et al., 2019). Deletion of the gene encoding p21, which is involved in cell cycle control downstream from p53, has been shown to rescue the proliferation defects observed in cultured mammary epithelial cells lacking β1 integrin (Li et al., 2005). Consistent with the data obtained *in vivo*, we found that: (1) clonogenicity of luminal progenitors was severely impaired after adenoCre-mediated depletion of LN-binding integrins *in vitro*; (2) the p53 pathway was activated in these cells, and depletion of p53 rescued the mammosphere formation capacity of α3α6KO luminal progenitors; and (3) as previously found in basal cells (Romagnoli et al., 2019), a Rho/ROCK/myosin II axis contributed to the activation of p53 pathway in the luminal progenitors depleted of LN-binding integrins.

Importantly, despite the restoration of hormone-induced alveologenesis by p53 inactivation in α3α6KO mice, milk protein transcript levels remained low, indicating that, as suggested by pioneering *in vitro* studies from Bissell's group, LN-binding integrins are essential for lactogenic differentiation (Muschler et al., 1999).

Surprisingly, at the onset of lactation, mammary glands in which the luminal cells lacked LN-binding integrins appeared to be well developed and functional. The altered morphology of the alveolar myoepithelial cells observed in mutant mice might provide an explanation for this. Indeed, the alveolar myoepithelial cells from α3α6KO mice were more spread out at the onset of lactation than control basal cells, limiting the contact of α3α6-integrin-depleted luminal cells with the basement membrane. RNAseq analysis showed that myoepithelial cells from α3α6KO mice displayed changes in the expression of genes involved in the regulation of cell adhesion and actin dynamics that might account for the observed alteration of cell shape. These findings suggest that cellular compensation mechanisms involving basal myoepithelial cells may contribute to the maintenance of alveolar architecture in α3α6KO mice. One possible explanation for the changes in myoepithelial cell phenotype would be a strengthening of their interactions with luminal cells depleted of LN-binding integrins as cell-cell and cell-ECM adhesions have been reported to exert negative feedback on each other (Burute and Thery, 2012). Another hypothetic mechanism could involve the tension forces exerted by the stroma on alveolar cells and mechano-transduction via cell-ECM adhesions including integrins (Glukhova and Streuli, 2013). Indeed, in normal alveoli, stroma exerts tension on both luminal and myoepithelial cells, while in α3α6KO glands, luminal cells lacking LN-binding integrins, forces might be redistributed on the myoepithelial cells, inducing their cytoskeletal changes.

We found that α3α6KO mice were unable to sustain lactation up to day 21, and by day 14, the pups fed by these mutant mice were already significantly lighter than those fed by control mice. By day 21, the glands from mutant females presented signs of premature involution, with collapsed alveoli and detached secretory cells in the lumen.

The interaction of integrin receptors with LN is known to be essential for the establishment of epithelial cell baso-apical polarity (reviewed by Lee and Streuli, 2014). Consistently, in α3α6KO females, by day 14 of lactation, numerous luminal cells had an aberrant morphology. These cells were not flattened like those in control tissues, and displayed signs of a disruption of baso-apical polarity, with mislocalized Par3 and E-cadherin, and dispersed or basally localized Golgi. These data suggest that milk secretion was impaired in α3α6KO females at peak lactation, as the formation and secretion of milk vesicles requires normal Golgi function and luminal cell polarization (Truchet and Honvo-Houéto, 2017). Importantly, in α3α6p53KO 14-day-lactating glands, morphological and polarity defects were also detected in luminal cells concomitantly with perturbed lactogenic gland differentiation.

In their seminal work, Streuli's team reported that the basement membrane was essential for the survival of mammary epithelial cells (Pullan et al., 1996). Consistent with this finding, we previously showed that the expression of a dominant-negative β1-integrin mutant induced apoptosis early in lactation (Faraldo et al., 1998). In α3α6KO mice, morphological alterations were visible in alveolar luminal cells at 14 days of lactation, but increases in apoptosis and lysosome/cathepsin-associated cell death were not detected in the mutant glands until day 21 of lactation, when the mutant glands began to undergo unscheduled involution. Notably,

Development (2020) 147, dev181552. doi:10.1242/dev.181552

the apoptosis observed in late lactation in α3α6KO females was completely abolished by p53 gene deletion, consistent with the proposed role for p53 in the triggering of cell death during the first few days of mammary involution (Jerry et al., 2002, 1998). The occurrence of cathepsin-associated cell death, reported by Watson's team to be the major cell death mechanism induced by milk stasis during post-lactation involution, is consistent with an impairment of milk secretion in mutant glands (Sargeant et al., 2014).

Klinowska et al. have reported that lobulo-alveolar development could occur in the absence of α3 or α6 chain-containing integrins, although that study did not present any quantitative evaluation of lactogenic differentiation in mutant epithelium (Klinowska et al., 2001). Consistently, we found that mammary glands depleted in luminal cells of α3 integrin appeared normal, whereas α6 depletion led to mild gland hypoplasia with a minor, but measurable, decrease in lactational differentiation. Only the simultaneous depletion of both the α3 and α6 integrins led to a significant perturbation of mammary development and function. The difference in phenotypes following the deletion of α3 or α6 alone is consistent with the non-redundant cellular functions of these integrins. Indeed, unlike α3, α6 can associate with β4, and the α6β4 dimer, unlike β1-containing integrins, is a component of hemidesmosomes. A recent study reported that deletion of β4 integrin from luminal cells induced defects in alveologenesis and milk production during pregnancy (Walker et al., 2020). Thus, the decreased β4-integrin surface levels detected in α3α6KO luminal cells could contribute to the observed phenotype.

We previously showed that α3 integrin is essential for the contractile function of basal myoepithelial cells during lactation (Raymond et al., 2011). These previously described mutant mice depleted of α3β1 integrin in the basal mammary epithelial layer, displayed milk stasis and their glands were engorged with milk. Importantly, in α3α6KO animals presenting integrin deletion in luminal compartment only, milk stasis was not observed, strongly indicating that apparently, the contractile activity was not perturbed in the myoepithelial cells of α3α6KO mice.

Previous studies have shown that the depletion of β1 integrins or the disruption of their function by the expression of a dominant-negative mutant in mammary luminal cells affects gland growth and differentiation (Faraldo et al., 1998; Li et al., 2005; Naylor et al., 2005). The mammary phenotype observed in mice in which the luminal cells were depleted of β1-integrins was more severe that the one observed here, with the mutant mice frequently unable to feed normal-size litters and, in the most extreme cases, total lactation failure. The β1-integrin subunit forms dimers with several different α subunits. Its depletion would therefore be expected to affect receptors not only for LN, but also for other ECM proteins, such as fibronectin, which has been shown to be essential for lobuloalveolar differentiation during pregnancy (Liu et al., 2010).

In recent decades, numerous studies have provided evidence for a role of LN-binding integrins in tumorigenesis, and both tumor-suppressing and tumor-promoting activities have been reported, depending on the cellular context (Ramovs et al., 2017). Importantly, luminal progenitors, the cell population targeted for integrin depletion in our model, are thought to be at the origin of basal-like breast tumors (Lim et al., 2009; Molyneux et al., 2010). In light of our data, it would be of interest to investigate the contribution of LN-binding integrins to basal-like breast cancer induction and progression, and, in particular, the contribution of these molecules to the regulation of cancer stem cells, which are often responsible for tumor relapse and, therefore, suitable therapeutic cell targets in this poor prognosis disease.

MATERIALS AND METHODS

Mice

The generation of *Itga3*$^{F/F}$, *Itga6*$^{F/F}$ and *Trp53*$^{F/F}$ mice has been previously described (De Arcangelis et al., 2017; Jonkers et al., 2001; Margadant et al., 2009). *BlgCre* transgenic mice were purchased from The Jackson Laboratory and the *Rosa26LacZ* reporter strain was kindly provided by Dr Soriano (Soriano, 1999). Mice were bred in a mixed CBA/C57Bl6 background. In all experiments *BlgCre*-negative littermates were used as controls. For pup weight measure, litters of eight pups were analyzed. The care and use of animals were conducted in accordance with the European and National Regulations for the Protection of Vertebrate Animals used for Experimental and other Scientific Purposes (facility license C750517/18). All experimental procedures were ethically approved (ethical approval 02265.02).

Whole-mount analyses, histology and immunolabeling

For whole-mount Carmine-Alum staining, dissected mammary fat pads were spread onto glass slides, fixed in a 1/3/6 mixture of acetic acid/chloroform/methanol and stained as described elsewhere (Teuliere et al., 2005). For whole-mount X-gal staining, mammary glands were fixed in 2.5% paraformaldehyde in PBS (pH 7.5), for 1 h at 4°C and stained overnight at 30°C (Biology of the Mammary Gland, mammary.nih.gov). For histological analyses, glands were embedded in paraffin wax, and 7 µm sections were cut and de-waxed for Fast Red counterstaining (X-gal-stained whole-mount glands), Hematoxylin/Eosin staining or immunolabeling. For alveolar density estimation, the whole surface occupied by alveoli was compared with the total mammary tissue surface using ImageJ on micrographs of Hematoxylin/Eosin stained sections. For cryosections, glands were frozen on Tissu-Tek (Sakura) and thin (5 µm) or thick (30 µm) sections were obtained using a Leica Cryostat. Thick sections were used to calculate basal cell parameters in lactating glands using ImageJ. Basal cells were immunolabeled with anti-α-smooth muscle actin antibody and their surface was measured in at least 30 alveoli from three mice per genotype. Branch width of basal cells was measured at the proximal part of the branch. A total of at least 100 branches in three mice per genotype were evaluated. The following primary antibodies were used for immunolabeling: mouse monoclonal anti-α-smooth muscle actin (Sigma-Aldrich A2547, 1/200), anti-keratin 8 (Covance MMS-162P, 1/100) and anti-GM130 (BD Biosciences, 610823, 1/100); rat monoclonal anti-β4 integrin (BD Biosciences clone, 346-11A, 1/100), anti-α6 integrin (BioLegend clone GoH3, 1/200), anti-β1 integrin (Millipore MAB1997, 1/100) and anti-E-cadherin (Life Technologies, 1/250); rabbit polyclonal anti α3 integrin (141742; Sachs et al., 2006), anti-PR (Santa Cruz Biotechnology, 7208, 1/200), anti-pankeratin (Dako, Z0622, 1/100), anti-Par3 (Millipore, 07-330, 1/100), anti-Ki67 (Labvision/Neomarkers, 1/200) and anti-laminin 5 (a kind gift from M. Aumalley, University of Cologne, Germany); and goat polyclonal anti-cathepsin D (Sicgen AB0043, 1/100). Alexa-fluor-conjugated secondary antibodies (Molecular Probes) were used at 1/500 dilution. Image acquisition was performed using a Leica DM 6000B microscope or a Nikon confocal A1r microscope.

TUNEL analysis

For cell death analysis, glands were fixed in 4% paraformaldehyde in PBS (pH 7.5) overnight at 4°C. Paraffin sections (7 µm) were analyzed for TdT digoxygenin nick-end labeling with Apoptag Plus (Sigma-Aldrich) following the manufacturer's instructions. After counterstaining with Methyl Green, 1500-2000 cells nuclei/sample were counted.

Mammary gland dissociation, cell sorting and flow cytometry analysis

Thoracic and inguinal mammary glands were pooled, dissociated and processed for single-cell suspension and flow cytometry as described elsewhere (Di-Cicco et al., 2015; Stingl et al., 2006; Taddei et al., 2008). For cell sorting, cells were incubated at 4°C for 20 min with the following antibodies: anti-CD45-APC (clone 30-F11), anti-CD31-APC (clone MEC13.3), anti-CD24-BViolet421 (clone M1/69), anti-CD49f-PeCy7 (clone GoH3), anti-ICAM1-PeCy7 (clone YN1/1.7.4) or anti-Sca-1-PE

Development (2020) 147, dev181552. doi:10.1242/dev.181552

(clone E13-161.7), all from BioLegend. Labeled cells were analyzed and sorted out using a MoFlo Astrios cell sorter (Beckman Coulter). Sorted luminal progenitor cells (CD31/45$^-$, CD24^{high} CD49f^{low} ICAM$^+$ population) were used for mammosphere assays and gene expression analysis. Sorted cell population purity was at least 95%. The antibodies used for the analysis of cell surface integrin expression in basal and luminal cells are presented in Table S2. Data were analyzed using FlowJo software.

Estrogen/progesterone stimulation experiments

For hormone stimulation, estrogen/progesterone silicon implants (E/P) from Belma Technologies were subcutaneously implanted into 12-week-old virgin females as previously described (Rajkumar et al., 2007). After 30 days, mammary glands 1 and 2 were collected for whole-mount Carmine staining and histological analyses, while glands 3, 4 and 5 were pooled for dissociation and cell sorting, as described below.

Organoids and mammospheres cell culture

Mammary organoids obtained as previously described (Ewald et al., 2008) were resuspended in Growth Factor Reduced Matrigel (BD Biosciences) and grown in 8-well coverslip bottom chambers (Ibidi). A suspension containing 300 organoids in 30 µl of Matrigel was added to each well. After 30 min at 37°C, minimal media was added: DMEM/F12, 1% v/v insulin, transferring, selenium (Sigma-Aldrich) and 1% penicillin/streptomycin. When indicated, prolactin (R&D Systems, 40 nM) or bFGF (GIBCO, 5 nM) was added to the medium after 1-2 h of culture and the medium was renewed every 2 days. Organoids were imaged using a Nikon Ni-E microscope, immunolabeled and visualized in a Nikon confocal A1r microscope or collected and analyzed for gene expression as indicated above.

For mammosphere cultures, freshly isolated luminal cells were seeded on ultralow-adherence 24-well plates (Corning) at the density of 10,000 cells/well, in mammosphere media: DMEM/F12 medium supplemented with B27 diluted 1/50 (Gibco), 20 ng/ml EGF (Invitrogen), 20 ng/ml bFGF (GIBCO), 4 µg/ml heparin (Sigma-Aldrich), 10 µg/ml insulin (Sigma-Aldrich) and 2% Matrigel (BD Pharmingen) as described previously (Chiche et al., 2013). After 12-14 days of culture, wells were photographed and mammospheres counted using ImageJ software then collected for RNA extraction and gene expression analysis.

Adeno-Cre mediated gene deletion

Freshly sorted luminal progenitor cells (CD31/45$^-$, CD24^{high} CD49f^{low} ICAM$^+$ population) were incubated with an adenovirus expressing the Cre recombinase under the control of the CMV promotor (AdCre, SignaGen Laboratories) at MOI of 4000 for 1 h at 37°C. After washing, cells were resuspended in mammosphere medium at the density of 7000 cells/well. For ROCK or myosin II-ATP-ase inhibition, Y27632 (1 µM, Millipore) or blebbistatin (5 µM, R&D Systems) were added to the mammosphere medium and replenished twice a week. After 12 days of culture, wells were photographed and the number of mammospheres was analyzed using ImageJ software.

Western blot analysis

Mammary tissue samples were homogenized in RIPA extraction buffer [40 mM Tris (pH 7.5), 276 mM NaCl, 2% Nonidet P-40, 4 mM EDTA] in the presence of protease and phosphatase inhibitors (ThermoScientific) following further incubation for 20 min at 4°C in a rotation wheel. A BCA Protein Assay (Pierce) was used to estimate protein concentration. Protein extracts (50 µg) were boiled for 5 min in Laemmli buffer before migration. Mammosphere pellets were resuspended in 1.5× hot Laemmli buffer, vortexed and boiled for 5 min. Samples were run on NuPAGE Novex 4-12% Bis Tris gels (Life Technologies/Invitrogen) and transferred onto nitrocellulose. Membranes were incubated with 5% BSA in TBS containing 0.1% Tween 20 (TBST) for 1 h at room temperature and with primary antibodies overnight at 4°C. The following primary antibodies were used: anti-p53 (clone 1C12, Cell Signaling Technologies), anti-MDM2 (clone EP16627; Abcam), anti-P-FAK-Tyr397 (Cell Signaling Technologies), anti-FAK (BD Transduction Laboratories), anti-P-MLC-Ser19, anti-MLC (Cell Signaling Technologies) and anti-GAPDH (clone FL-335, Santa Cruz Biotechnology). Secondary antibodies coupled to horseradish peroxidase were from Cell Signaling Technologies. Detection was performed by chemiluminescence (Super Signal West Pico+, Pierce). Quantitative analysis was performed with ImageJ.

RNA extraction and RT-qPCR

RNA was isolated from whole mammary glands using Trizol reagent (Life Technologies) and further purified on a cleanup column (Qiagen). For mammosphere and organoid RNA extraction, RNeasy Microkit was used. To avoid eventual DNA contamination, purified RNA was treated with DNAse (Qiagen). RNAs were reverse-transcribed using MMLV H(−) Point reverse transcriptase (Promega). Quantitative PCR was performed using the QuantiNova SYBR Green PCR Kit (Qiagen) on a LightCycler 480 real-time PCR system (Roche). The values obtained were normalized to *Gapdh* levels. The primers used for RT-qPCR analysis were purchased from SABiosciences/Qiagen or designed using Oligo 6.8 software (Molecular Biology Insights) and synthesized by Eurogentec. Primers used in this study are listed in Table S3.

Microarray analysis

Global gene expression analysis was performed with total RNA extracted from sorted luminal cells. RNA quality control was performed with an Agilent 2100 Bioanalyzer (Agilent Technologies). The WT-Ovation Pico RNA Amplification system (Nugen) was used on 1 ng of total RNA to generate sufficient amount of biotinylated cDNA. Samples were hybridized on Affymetrix GeneChip Mouse Genome ClariomS arrays. Analyses were made using EASANA (GenoSplice, www.genosplice.com), which is based on the GenoSplice FAST DB release 2014_2 annotations (de la Grange et al., 2005). Data were normalized using quantile normalization and an unpaired Student's *t*-test was used to compare gene intensities in the different samples. Genes were considered significantly regulated when fold-change between the compared groups was at least 1.5 and uncorrected *P*-value was equal to or less than 0.05. The molecular and functional interactions of the genes identified were analyzed with REACTOME pathway analysis. The microarray data are available in GEO under accession number GSE132349.

RNA sequencing

cDNA was generated from total RNA by the SMART-seq V4 Ultra-low input kit, subjected to quality control on a BioAnalyzer and accurately quantified using a Qubit fluorometer. Libraries were prepared from 0.6 ng of cDNA using the Illumina Nextera XT library preparation kit according to the manufacturer's instructions. Sequencing was carried out using 2×100 cycles (paired-end reads, 100 nucleotides) on an Illumina HiSeq2500 instrument (rapid flow cells) to obtain around 20 M paired reads per sample. Quality assessment on data confirmed good complexity of libraries and low duplicate rate (less than 10%). RNA-seq data analysis was performed by GenoSplice technology (www.genosplice.com). Sequencing, data quality, reads repartition and insert size estimation were performed using FastQC, Picard-Tools, Samtools and rseqc. Reads were mapped using STARv2.4.0 on the mm10 Mouse genome assembly (Dobin et al., 2013). Normalization and differential gene expression were performed using DESeq2 (Love et al., 2014) on R (v.3.1.3). Genes were considered as expressed if their rpkm value was greater than 97.5% of the background rpkm value based on intergenic regions. Results were considered statistically significant for unadjusted *P*-values equal to or less than 0.05 and fold-changes of at least 1.5. The RNA-seq data are available in GEO under accession number GSE132281.

Statistical analysis

All values are shown as mean±s.d. *P*-values were determined using Student's *t*-test with two-tailed distribution and unequal variance (Welch's correction). All statistical analyses were performed using GraphPad Prism v6 software.

Acknowledgements

We are particularly grateful to C. Lambert for technical assistance, to Dr I. Grandjean, S. Jannet and the personnel of the animal facilities at Institut Curie for taking care of the mice, to Z. Maciorowski, A. Viguier and S. Grondin for excellent assistance with FACS analyses, and to the Cell and Tissue Imaging (PICT-IBiSA),

Institut Curie, member of the French National Research Infrastructure France-BioImaging (ANR10-INBS-04). We also thank Drs K. Raymond and S. Cagnet for obtaining mice, Drs P. Soriano and J. Jonkers for providing mouse strains, and Dr K. Raymond for helpful discussion. High-throughput sequencing was performed by the ICGex NGS platform of the Institut Curie supported by grants ANR-10-EQPX-03 and ANR-10-INBS-09-0, and by the Cancéropole Ile-de-France (INCa-DGOS-4654).

Competing interests
The authors declare no competing or financial interests.

Author contributions
Conceptualization: M.R., M.A.G., M.M.F.; Methodology: M.R., L.B., S.B., P.d.I.G., M.-A.D., M.A.G., M.M.F.; Investigation: M.R., L.B., A.D.-C, M.P.-L., P.L., S.B., P.d.I.G., M.-A.D., M.M.F.; Resources: A.D.A., E.G.-L., A.S.; Writing - original draft: M.R., M.A.G., M.M.F.; Funding acquisition: M.R., M.-A.D., M.A.G., M.M.F.

Funding
The work was supported by grants from the Agence Nationale de la Recherche (ANR-13-BSV2-0001), the Institut National Du Cancer (2014-1-SEIN-01-ICR-1), the Agence Nationale de la Recherche and the Ligue Contre le Cancer Ile de France (Comité de Paris RS16/75-70 and RS19/75-67; Comité de l'Essonne, M27216) and Labex Celtisphybio (ANR-10-LABX-0038), part of the Idex PSL. M.R. received funding from the Marie Curie Fellowship Program.

Data availability
The microarray data have been deposited in GEO under accession number GSE132349. The RNAseq data have been deposited in GEO under accession number GSE132281.

Supplementary information
Supplementary information available online at
http://dev.biologists.org/lookup/doi/10.1242/dev.181552.supplemental

References
Asselin-Labat, M.-L., Sutherland, K. D., Barker, H., Thomas, R., Shackleton, M., Forrest, N. C., Hartley, L., Robb, L., Grosveld, F. G., van der Wees, J. et al. (2007). Gata-3 is an essential regulator of mammary-gland morphogenesis and luminal-cell differentiation. *Nat. Cell Biol.* **9**, 201-209. doi:10.1038/ncb1530

Barczyk, M., Carracedo, S. and Gullberg, D. (2010). Integrins. *Cell Tissue Res.* **339**, 269-280. doi:10.1007/s00441-009-0834-6

Blaas, L., Pucci, F., Messal, H. A., Andersson, A. B., Josue Ruiz, E., Gerling, M., Douagi, I., Spencer-Dene, B., Musch, A., Mitter, R. et al. (2016). Lgr6 labels a rare population of mammary gland progenitor cells that are able to originate luminal mammary tumours. *Nat. Cell Biol.* **18**, 1346-1356. doi:10.1038/ncb3434

Brisken, C. and Ataca, D. (2015). Endocrine hormones and local signals during the development of the mouse mammary gland. *Wiley Interdiscip. Rev. Dev. Biol.* **4**, 181-195. doi:10.1002/wdev.172

Brisken, C. and O'Malley, B. (2010). Hormone action in the mammary gland. *Cold Spring Harb. Perspect. Biol.* **2**, a003178. doi:10.1101/cshperspect.a003178

Burute, M. and Thery, M. (2012). Spatial segregation between cell-cell and cell-matrix adhesions. *Curr. Opin. Cell Biol.* **24**, 628-636. doi:10.1016/j.ceb.2012.07.003

Carr, M. I. and Jones, S. N. (2016). Regulation of the Mdm2-p53 signaling axis in the DNA damage response and tumorigenesis. *Transl. Cancer Res.* **5**, 707-724. doi:10.21037/tcr.2016.11.75

Chiche, A., Moumen, M., Petit, V., Jonkers, J., Medina, D., Deugnier, M.-A., Faraldo, M. M. and Glukhova, M. A. (2013). Somatic loss of p53 leads to stem/progenitor cell amplification in both mammary epithelial compartments, basal and luminal. *Stem Cells* **31**, 1857-1867. doi:10.1002/stem.1429

Chiche, A., Di-Cicco, A., Sesma-Sanz, L., Bresson, L., de la Grange, P., Glukhova, M. A., Faraldo, M. M. and Deugnier, M.-A. (2019). p53 controls the plasticity of mammary luminal progenitor cells downstream of Met signaling. *Breast Cancer Res.* **21**, 13. doi:10.1186/s13058-019-1101-8

De Arcangelis, A., Hamade, H., Alpy, F., Normand, S., Bruyère, E., Lefebvre, O., Méchine-Neuville, A., Siebert, S., Pfister, V., Lepage, P. et al. (2017). Hemidesmosome integrity protects the colon against colitis and colorectal cancer. *Gut* **66**, 1748-1760. doi:10.1136/gutjnl-2015-310847

de la Grange, P., Dutertre, M., Martin, N. and Auboeuf, D. (2005). FAST DB: a website resource for the study of the expression regulation of human gene products. *Nucleic Acids Res.* **33**, 4276-4284. doi:10.1093/nar/gki738

Di-Cicco, A., Petit, V., Chiche, A., Bresson, L., Romagnoli, M., Orian-Rousseau, V., Vivanco, M. d. M., Medina, D., Faraldo, M. M., Glukhova, M. A. et al. (2015). Paracrine Met signaling triggers epithelial-mesenchymal transition in mammary luminal progenitors, affecting their fate. *eLife* **4**, e06104. doi:10.7554/eLife.06104

Dobin, A., Davis, C. A., Schlesinger, F., Drenkow, J., Zaleski, C., Jha, S., Batut, P., Chaisson, M. and Gingeras, T. R. (2013). STAR: ultrafast universal RNA-seq aligner. *Bioinformatics* **29**, 15-21. doi:10.1093/bioinformatics/bts635

Elias, S., Morgan, M. A., Bikoff, E. K. and Robertson, E. J. (2017). Long-lived unipotent Blimp1-positive luminal stem cells drive mammary gland organogenesis throughout adult life. *Nat. Commun.* **8**, 1714. doi:10.1038/s41467-017-01971-w

Ewald, A. J., Brenot, A., Duong, M., Chan, B. S. and Werb, Z. (2008). Collective epithelial migration and cell rearrangements drive mammary branching morphogenesis. *Dev. Cell* **14**, 570-581. doi:10.1016/j.devcel.2008.03.003

Faraldo, M. M., Deugnier, M. A., Lukashev, M., Thiery, J. P. and Glukhova, M. A. (1998). Perturbation of beta1-integrin function alters the development of murine mammary gland. *EMBO J.* **17**, 2139-2147. doi:10.1093/emboj/17.8.2139

Faraldo, M. M., Deugnier, M.-A., Tlouzeau, S., Thiery, J. P. and Glukhova, M. A. (2002). Perturbation of β1-integrin function in involuting mammary gland results in premature dedifferentiation of secretory epithelial cells. *Mol. Biol. Cell* **13**, 3521-3531. doi:10.1091/mbc.e02-02-0086

Fernandez-Valdivia, R., Mukherjee, A., Ying, Y., Li, J., Paquet, M., DeMayo, F. J. and Lydon, J. P. (2009). The RANKL signaling axis is sufficient to elicit ductal side-branching and alveologenesis in the mammary gland of the virgin mouse. *Dev. Biol.* **328**, 127-139. doi:10.1016/j.ydbio.2009.01.019

Glukhova, M. A. and Streuli, C. H. (2013). How integrins control breast biology. *Curr. Opin. Cell Biol.* **25**, 633-641. doi:10.1016/j.ceb.2013.06.010

Hynes, R. O. (2002). Integrins: bidirectional, allosteric signaling machines. *Cell* **110**, 673-687. doi:10.1016/S0092-8674(02)00971-6

Jerry, D. J., Kuperwasser, C., Downing, S. R., Pinkas, J., He, C., Dickinson, E., Marconi, S. and Naber, S. P. (1998). Delayed involution of the mammary epithelium in BALB/c-p53null mice. *Oncogene* **17**, 2305-2312. doi:10.1038/sj.onc.1202157

Jerry, D. J., Dickinson, E. S., Roberts, A. L. and Said, T. K. (2002). Regulation of apoptosis during mammary involution by the p53 tumor suppressor gene. *J. Dairy Sci.* **85**, 1103-1110. doi:10.3168/jds.S0022-0302(02)74171-4

Jonkers, J., Meuwissen, R., van der Gulden, H., Peterse, H., van der Valk, M. and Berns, A. (2001). Synergistic tumor suppressor activity of BRCA2 and p53 in a conditional mouse model for breast cancer. *Nat. Genet.* **29**, 418-425. doi:10.1038/ng747

Klinowska, T. C. M., Alexander, C. M., Georges-Labouesse, E., Van der Neut, R., Kreidberg, J. A., Jones, C. J. P., Sonnenberg, A. and Streuli, C. H. (2001). Epithelial development and differentiation in the mammary gland is not dependent on α3 or α6 integrin subunits. *Dev. Biol.* **233**, 449-467. doi:10.1006/dbio.2001.0204

Kritikou, E. A., Sharkey, A., Abell, K., Came, P. J., Anderson, E., Clarkson, R. W. E. and Watson, C. J. (2003). A dual, non-redundant, role for LIF as a regulator of development and STAT3-mediated cell death in mammary gland. *Development* **130**, 3459-3468. doi:10.1242/dev.00578

Lee, J. L. and Streuli, C. H. (2014). Integrins and epithelial cell polarity. *J. Cell Sci.* **127**, 3217-3225. doi:10.1242/jcs.146142

Li, N., Zhang, Y., Naylor, M. J., Schatzmann, F., Maurer, F., Wintermantel, T., Schuetz, G., Mueller, U., Streuli, C. H. and Hynes, N. E. (2005). β1 integrins regulate mammary gland proliferation and maintain the integrity of mammary alveoli. *EMBO J.* **24**, 1942-1953. doi:10.1038/sj.emboj.7600674

Lim, E., Vaillant, F., Wu, D., Forrest, N. C., Pal, B., Hart, A. H., Asselin-Labat, M.-L., Gyorki, D. E., Ward, T., Partanen, A. et al. (2009). Aberrant luminal progenitors as the candidate target population for basal tumor development in BRCA1 mutation carriers. *Nat. Med.* **15**, 907-913. doi:10.1038/nm.2000

Liu, K., Cheng, L., Flesken-Nikitin, A., Huang, L., Nikitin, A. Y. and Pauli, B. U. (2010). Conditional knockout of fibronectin abrogates mouse mammary gland lobuloalveolar differentiation. *Dev. Biol.* **346**, 11-24. doi:10.1016/j.ydbio.2010.07.001

Love, M. I., Huber, W. and Anders, S. (2014). Moderated estimation of fold change and dispersion for RNA-seq data with DESeq2. *Genome Biol.* **15**, 550. doi:10.1186/s13059-014-0550-8

Macias, H. and Hinck, L. (2012). Mammary gland development. *Wiley Interdiscip. Rev. Dev. Biol.* **1**, 533-557. doi:10.1002/wdev.35

Margadant, C., Raymond, K., Kreft, M., Sachs, N., Janssen, H. and Sonnenberg, A. (2009). Integrin α3β1 inhibits directional migration and wound re-epithelialization in the skin. *J. Cell Sci.* **122**, 278-288. doi:10.1242/jcs.029108

Molyneux, G., Geyer, F. C., Magnay, F.-A., McCarthy, A., Kendrick, H., Natrajan, R., Mackay, A., Grigoriadis, A., Tutt, A., Ashworth, A. et al. (2010). BRCA1 basal-like breast cancers originate from luminal epithelial progenitors and not from basal stem cells. *Cell Stem Cell* **7**, 403-417. doi:10.1016/j.stem.2010.07.010

Muschler, J. and Streuli, C. H. (2010). Cell-matrix interactions in mammary gland development and breast cancer. *Cold Spring Harb. Perspect. Biol.* **2**, a003202. doi:10.1101/cshperspect.a003202

Muschler, J., Lochter, A., Roskelley, C. D., Yurchenco, P. and Bissell, M. J. (1999). Division of labor among the α6β4 integrin, β1 integrins, and an E3 laminin receptor to signal morphogenesis and β-casein expression in mammary epithelial cells. *Mol. Biol. Cell* **10**, 2817-2828. doi:10.1091/mbc.10.9.2817

Naylor, M. J., Li, N., Cheung, J., Lowe, E. T., Lambert, E., Marlow, R., Wang, P., Schatzmann, F., Wintermantel, T., Schüetz, G. et al. (2005). Ablation of β1 integrin in mammary epithelium reveals a key role for integrin in glandular

morphogenesis and differentiation. *J. Cell Biol.* **171**, 717-728. doi:10.1083/jcb.200503144

Pullan, S., Wilson, J., Metcalfe, A., Edwards, G. M., Goberdhan, N., Tilly, J., Hickman, J. A., Dive, C. and Streuli, C. H. (1996). Requirement of basement membrane for the suppression of programmed cell death in mammary epithelium. *J. Cell Sci.* **109**, 631-642.

Rajkumar, L., Kittrell, F. S., Guzman, R. C., Brown, P. H., Nandi, S. and Medina, D. (2007). Hormone-induced protection of mammary tumorigenesis in genetically engineered mouse models. *Breast Cancer Res.* **9**, R12. doi:10.1186/bcr1645

Ramovs, V., te Molder, L. and Sonnenberg, A. (2017). The opposing roles of laminin-binding integrins in cancer. *Matrix Biol.* **57-58**, 213-243. doi:10.1016/j.matbio.2016.08.007

Raymond, K., Cagnet, S., Kreft, M., Janssen, H., Sonnenberg, A. and Glukhova, M. A. (2011). Control of mammary myoepithelial cell contractile function by α3β1 integrin signalling. *EMBO J.* **30**, 1896-1906. doi:10.1038/emboj.2011.113

Raymond, K., Faraldo, M. M., Deugnier, M.-A. and Glukhova, M. A. (2012). Integrins in mammary development. *Semin. Cell Dev. Biol.* **23**, 599-605. doi:10.1016/j.semcdb.2012.03.008

Rios, A. C., Fu, N. Y., Lindeman, G. J. and Visvader, J. E. (2014). In situ identification of bipotent stem cells in the mammary gland. *Nature* **506**, 322-327. doi:10.1038/nature12948

Rodilla, V., Dasti, A., Huyghe, M., Lafkas, D., Laurent, C., Reyal, F. and Fre, S. (2015). Luminal progenitors restrict their lineage potential during mammary gland development. *PLoS Biol.* **13**, e1002069. doi:10.1371/journal.pbio.1002069

Romagnoli, M., Cagnet, S., Chiche, A., Bresson, L., Baulande, S., de la Grange, P., De Arcangelis, A., Kreft, M., Georges-Labouesse, E., Sonnenberg, A. et al. (2019). Deciphering the mammary stem cell niche: a role for laminin-binding integrins. *Stem Cell Rep.* **12**, 831-844. doi:10.1016/j.stemcr.2019.02.008

Sachs, N., Kreft, M., van den Bergh Weerman, M. A., Beynon, A. J., Peters, T. A., Weening, J. J. and Sonnenberg, A. (2006). Kidney failure in mice lacking the tetraspanin CD151. *J. Cell Biol.* **175**, 33-39. doi:10.1083/jcb.200603073

Sargeant, T. J., Lloyd-Lewis, B., Resemann, H. K., Ramos-Montoya, A., Skepper, J. and Watson, C. J. (2014). Stat3 controls cell death during mammary gland involution by regulating uptake of milk fat globules and lysosomal membrane permeabilization. *Nat. Cell Biol.* **16**, 1057-1068. doi:10.1038/ncb3043

Schere-Levy, C., Buggiano, V., Quaglino, A., Gattelli, A., Cirio, M. C., Piazzon, I., Vanzulli, S. and Kordon, E. C. (2003). Leukemia inhibitory factor induces apoptosis of the mammary epithelial cells and participates in mouse mammary gland involution. *Exp. Cell Res.* **282**, 35-47. doi:10.1006/excr.2002.5666

Selbert, S., Bentley, D. J., Melton, D. W., Rannie, D., Lourenço, P., Watson, C. J. and Clarke, A. R. (1998). Efficient BLG-Cre mediated gene deletion in the mammary gland. *Transgenic Res.* **7**, 387-396. doi:10.1023/a:1008848304391

Shackleton, M., Vaillant, F., Simpson, K. J., Stingl, J., Smyth, G. K., Asselin-Labat, M.-L., Wu, L., Lindeman, G. J. and Visvader, J. E. (2006). Generation of a functional mammary gland from a single stem cell. *Nature* **439**, 84-88. doi:10.1038/nature04372

Shehata, M., Teschendorff, A., Sharp, G., Novcic, N., Russell, I. A., Avril, S., Prater, M., Eirew, P., Caldas, C., Watson, C. J. et al. (2012). Phenotypic and functional characterisation of the luminal cell hierarchy of the mammary gland. *Breast Cancer Res.* **14**, R134. doi:10.1186/bcr3334

Sleeman, K. E., Kendrick, H., Robertson, D., Isacke, C. M., Ashworth, A. and Smalley, M. J. (2007). Dissociation of estrogen receptor expression and in vivo stem cell activity in the mammary gland. *J. Cell Biol.* **176**, 19-26. doi:10.1083/jcb.200604065

Soriano, P. (1999). Generalized lacZ expression with the ROSA26 Cre reporter strain. *Nat. Genet.* **21**, 70-71. doi:10.1038/5007

Stingl, J., Eirew, P., Ricketson, I., Shackleton, M., Vaillant, F., Choi, D., Li, H. I. and Eaves, C. J. (2006). Purification and unique properties of mammary epithelial stem cells. *Nature* **439**, 993-997. doi:10.1038/nature04496

Streuli, C. H., Schmidhauser, C., Bailey, N., Yurchenco, P., Skubitz, A. P., Roskelley, C. and Bissell, M. J. (1995). Laminin mediates tissue-specific gene expression in mammary epithelia. *J. Cell Biol.* **129**, 591-603. doi:10.1083/jcb.129.3.591

Taddei, I., Deugnier, M.-A., Faraldo, M. M., Petit, V., Bouvard, D., Medina, D., Fässler, R., Thiery, J. P. and Glukhova, M. A. (2008). β1 integrin deletion from the basal compartment of the mammary epithelium affects stem cells. *Nat. Cell Biol.* **10**, 716-722. doi:10.1038/ncb1734

Teuliere, J., Faraldo, M. M., Deugnier, M. A., Shtutman, M., Ben-Ze'ev, A., Thiery, J. P. and Glukhova, M. A. (2005). Targeted activation of β-catenin signaling in basal mammary epithelial cells affects mammary development and leads to hyperplasia. *Development* **132**, 267-277. doi:10.1242/dev.01583

Truchet, S. and Honvo-Houéto, E. (2017). Physiology of milk secretion. *Best Pract. Res. Clin. Endocrinol. Metab.* **31**, 367-384. doi:10.1016/j.beem.2017.10.008

Van Keymeulen, A., Rocha, A. S., Ousset, M., Beck, B., Bouvencourt, G., Rock, J., Sharma, N., Dekoninck, S. and Blanpain, C. (2011). Distinct stem cells contribute to mammary gland development and maintenance. *Nature* **479**, 189-193. doi:10.1038/nature10573

Van Keymeulen, A., Fioramonti, M., Centonze, A., Bouvencourt, G., Achouri, Y. and Blanpain, C. (2017). Lineage-restricted mammary stem cells sustain the development, homeostasis, and regeneration of the estrogen receptor positive lineage. *Cell Rep.* **20**, 1525-1532. doi:10.1016/j.celrep.2017.07.066

Visvader, J. E. and Smith, G. H. (2011). Murine mammary epithelial stem cells: discovery, function, and current status. *Cold Spring Harb. Perspect. Biol.* **3**, a004879. doi:10.1101/cshperspect.a004879

Walker, M. R., Amante, J. J., Li, J., Liu, H., Zhu, L. J., Feltri, M. L., Goel, H. L. and Mercurio, A. M. (2020). Alveolar progenitor cells in the mammary gland are dependent on the β4 integrin. *Dev. Biol.* **457**, 13-19. doi:10.1016/j.ydbio.2019.10.001

Wang, C., Christin, J. R., Oktay, M. H. and Guo, W. (2017). Lineage-biased stem cells maintain estrogen-receptor-positive and -negative mouse mammary luminal lineages. *Cell Rep.* **18**, 2825-2835. doi:10.1016/j.celrep.2017.02.071

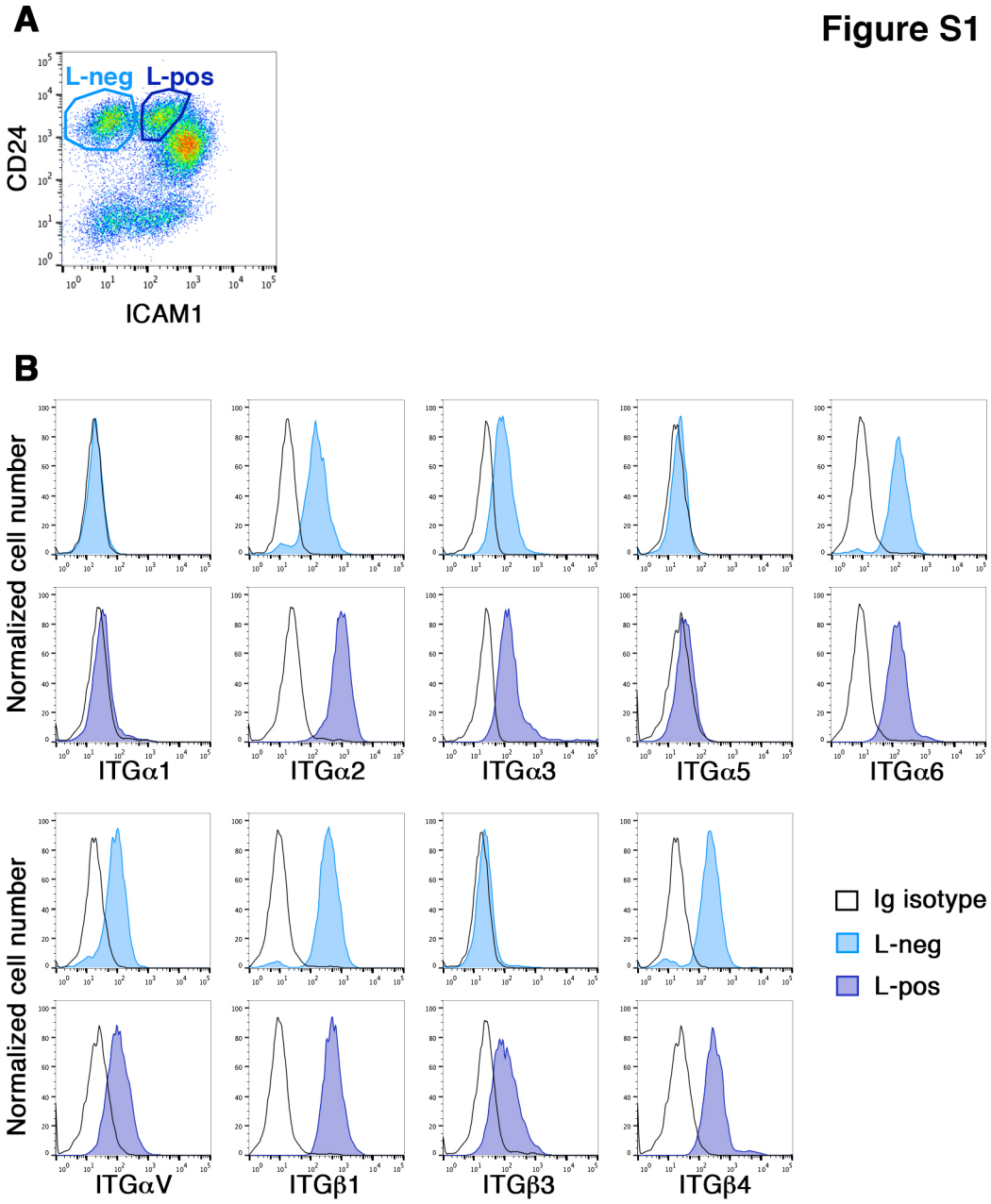

Figure S1. Analysis of integrin expression in freshly sorted mammary luminal cells from 16-weeks-old virgin mice. Related to Figure 1**.**

(A) Dot plot showing separation of luminal cell populations by flow cytometry on the basis of CD24 and ICAM1 expression. L-Neg: Luminal ICAM-negative population; L-pos: Luminal ICAM-positive (clonogenic) population.

(B) Flow cytometry analysis of integrin expression in L-Neg and L-pos cells separated as shown in (A).

Figure S2

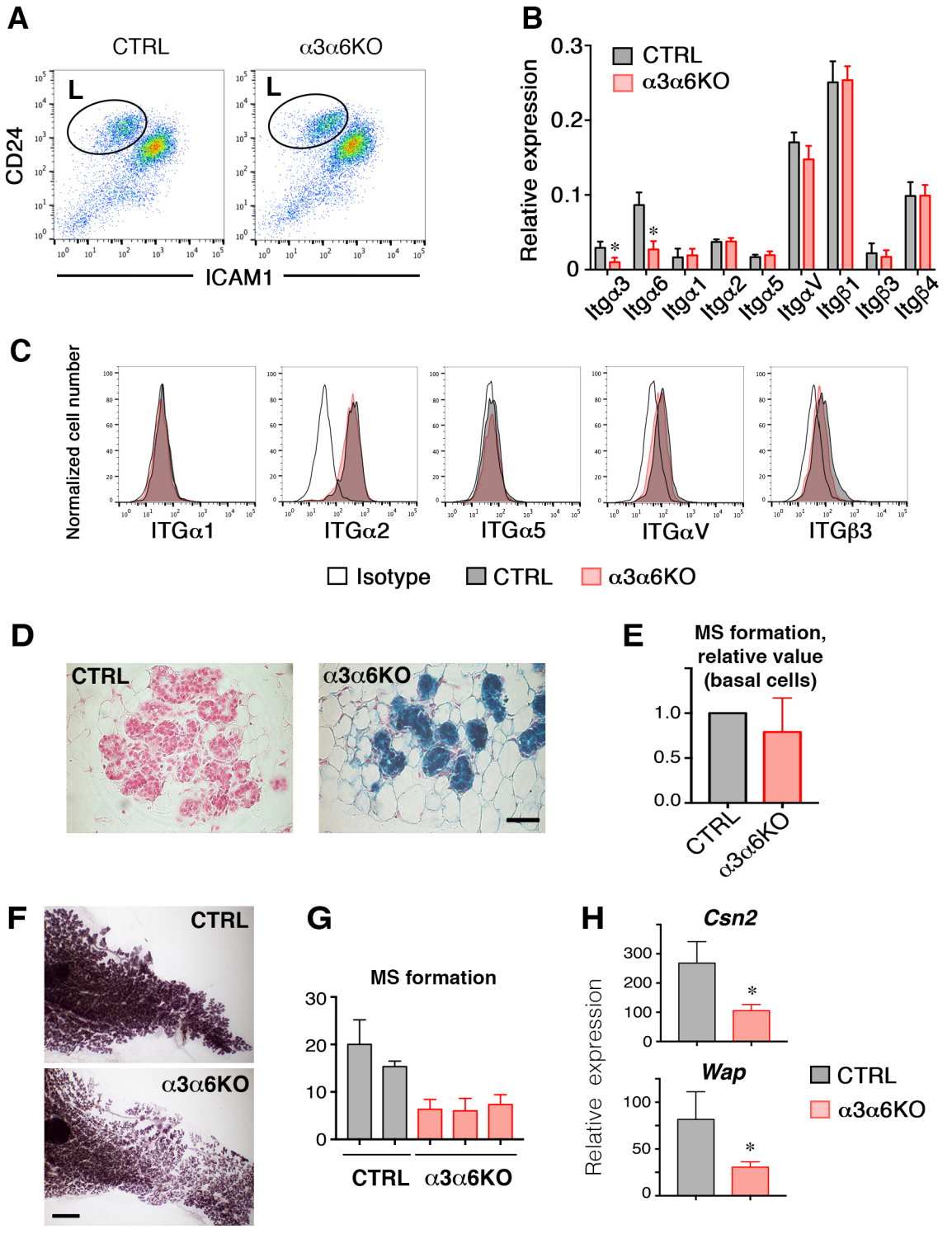

Figure S2. Analysis of integrin expression in mammary luminal cells isolated from 15-day-pregnant mice. Related to Figure 1.

(A) Dot plot showing separation of basal and luminal cells from 15-day-pregnant mammary glands by flow cytometry. L: luminal cells.

(B) RT-qPCR analysis of integrin gene expression in freshly isolated luminal cells sorted from 15-day-pregnant mammary glands as illustrated in A. The values were normalized to *Gapdh* and presented as means+SD from three independent experiments. p = 0.05 for *Itga3* and 0.03 for *Itga6*.

(C) Flow cytometry analysis of integrin expression in mammary luminal cells from control and α3α6KO females.

(D) Sections through 15-day-pregnant control and α3α6KO mouse mammary glands. X-gal staining. Bar, 40 μm.

(E) Mammosphere formation by basal cells sorted from 15-day-pregnant mouse mammary glands. The values shown are means±SD obtained in 3 independent experiments.

(F) 18-day-pregnant control and α3α6KO mammary glands stained with Carmine in whole-mount (bar, 2 mm).

(G) Mammosphere formation by luminal cells sorted from 18-day-pregnant mouse mammary glands. The values shown are means±SD of mammospheres obtained in 3 well replicates obtained with 10000 cells from two control and three α3α6KO females.

(H) RT-qPCR analysis of milk protein gene expression in freshly sorted luminal cells from 18-day-pregnant mouse mammary glands. The values shown are means±SD obtained from 4 control and 4 α3α6KO females. * p = 0.024 for *Csn2* and 0.048 for *Wap*.

Figure S3

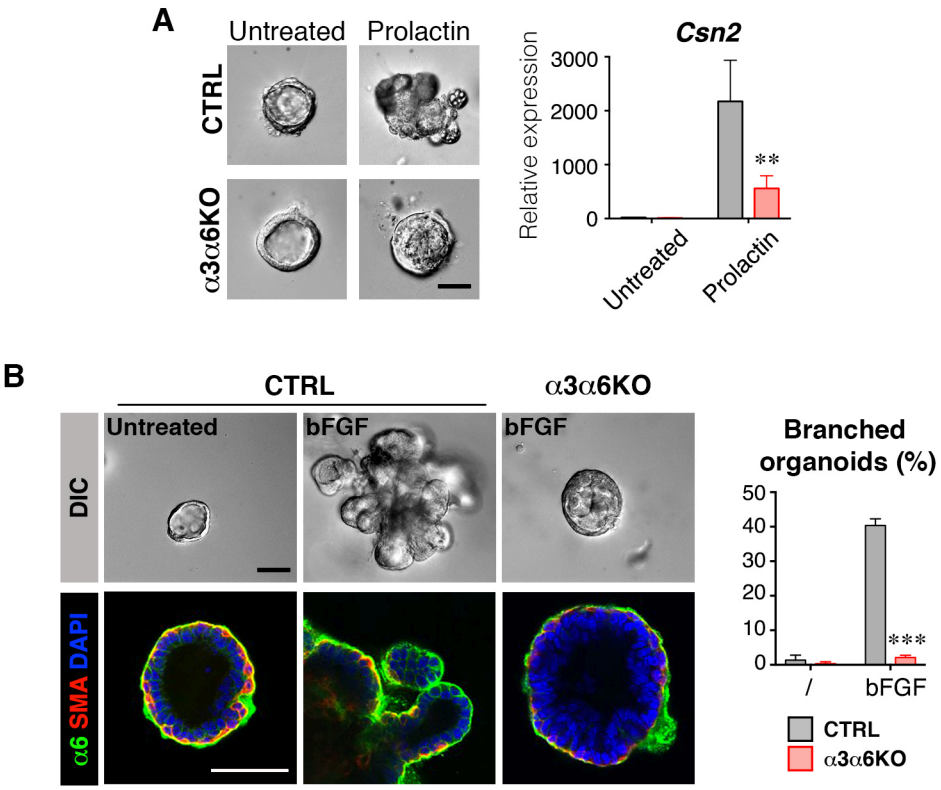

Figure S3. Analysis of mammary organoids obtained from 15-day-pregnant mammary glands. Related to Figure 1.

(A) Left: DIC images of mammary organoids after 10 days of culture in the presence or absence of prolactin. Bar, 30 μm. Right: RT-qPCR analysis of *Csn2* gene expression in mammary organoides cultured for 8-12 days in the presence or absence of prolactin. Means+SD from 4 independent experiments are shown. p = 0.007.

(B) Mammary organoids after 5 days of culture in the presence or absence of bFGF. Upper panels, representative contrast microscopy (DIC) images. Lower panels, immunofluorescence labeling with antibodies against α6 integrin and anti α-SMA, confocal microscopy. DAPI served to visualize nuclei. Bar, 30 μm in upper panels and 50 μm in lower panels. The graph represents the percentage of branched organoids (i.e., with 3 branches at least). Means+SD from three independent experiments are shown. p = 0.000005.

Figure S4

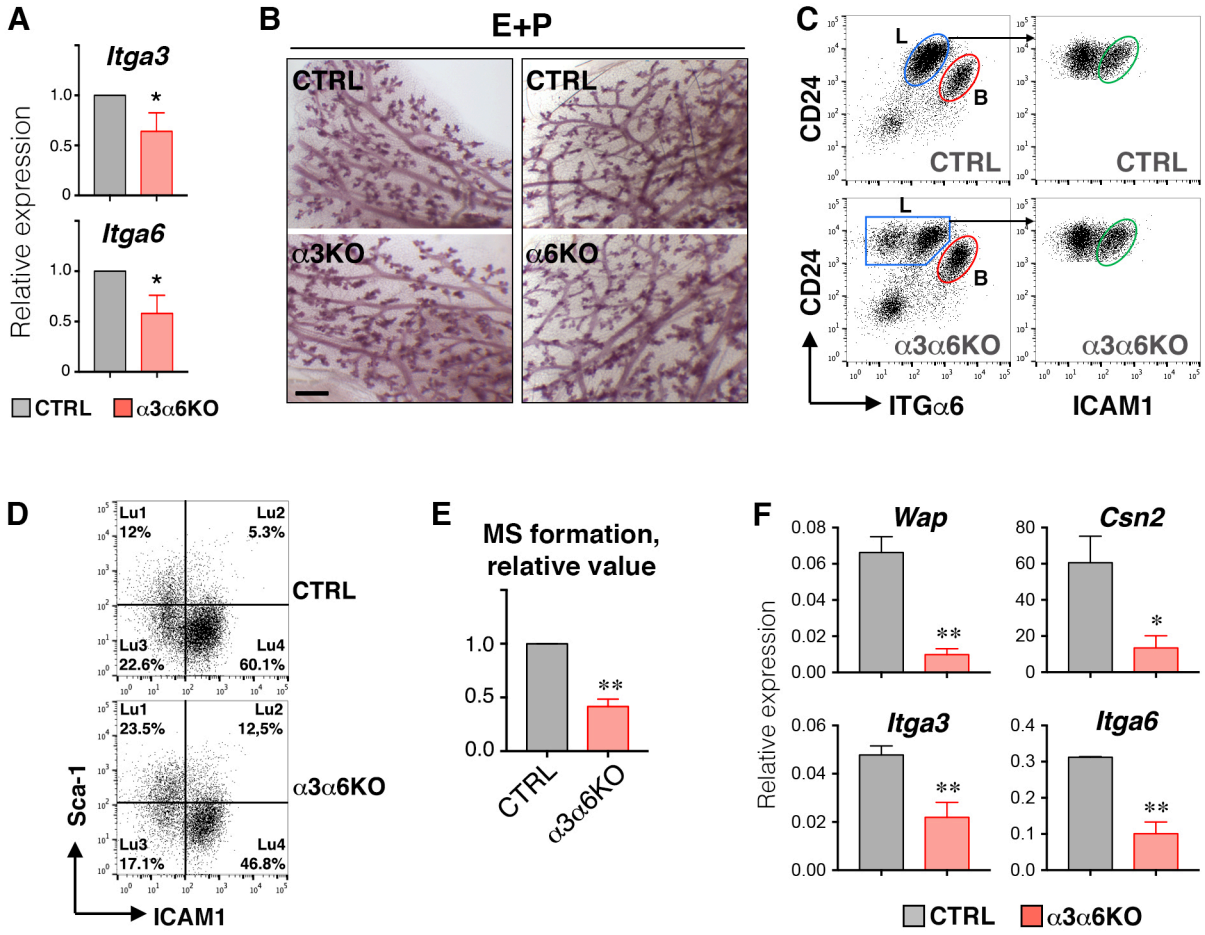

Figure S4. Effect of E/P stimulation on mammary glands. Related to Figure 2**.**

(A) RT-qPCR analysis of integrin gene expression in luminal cells sorted from mammary glands stimulated with E/P. The values were normalized to *Gapdh* and presented as means+SD from four independent experiments. p = 0.03 for *Itga3* and 0.02 for *Itga6*.

(B) Fragments of mammary glands from E/P-stimulated α3KO and α6KO and their respective control littermates stained with Carmine in whole-mounts. Bar, 400 μm.

(C) Dot plot showing flow cytometry separation of mammary epithelial cells from E/P stimulated mammary glands. Left panels, separation of basal and luminal cells. Right: Luminal cells where plotted for ICAM1 expression, and the ICAM1+ progenitor population (green circle) selected for further analyses (see Figure 2).

(D) Dot plot showing flow cytometry separation of mammary luminal cells from E/P stimulated mammary glands on the bases of their ICAM1 and Sca-1 expression. The cell percentage of each of the four populations (Lu1 to Lu4) is indicated. A representative experiment is shown.

(E) Mammosphere formation by Lu4 cells sorted from E/P stimulated mammary glands. The values shown are means±SD obtained in 3 independent experiments. p = 0.005.

(F) RT-qPCR analysis of milk protein and integrin gene expression in freshly sorted Lu4 cells from E/P stimulated mammary glands. The values shown are means±SD obtained from 3 control and 3 α3α6KO females. * p = 0.004 for *Wap*; 0.017 for *Csn2*; 0.006 for *Itga3;* 0.007 for *Itga6.*

Figure S5

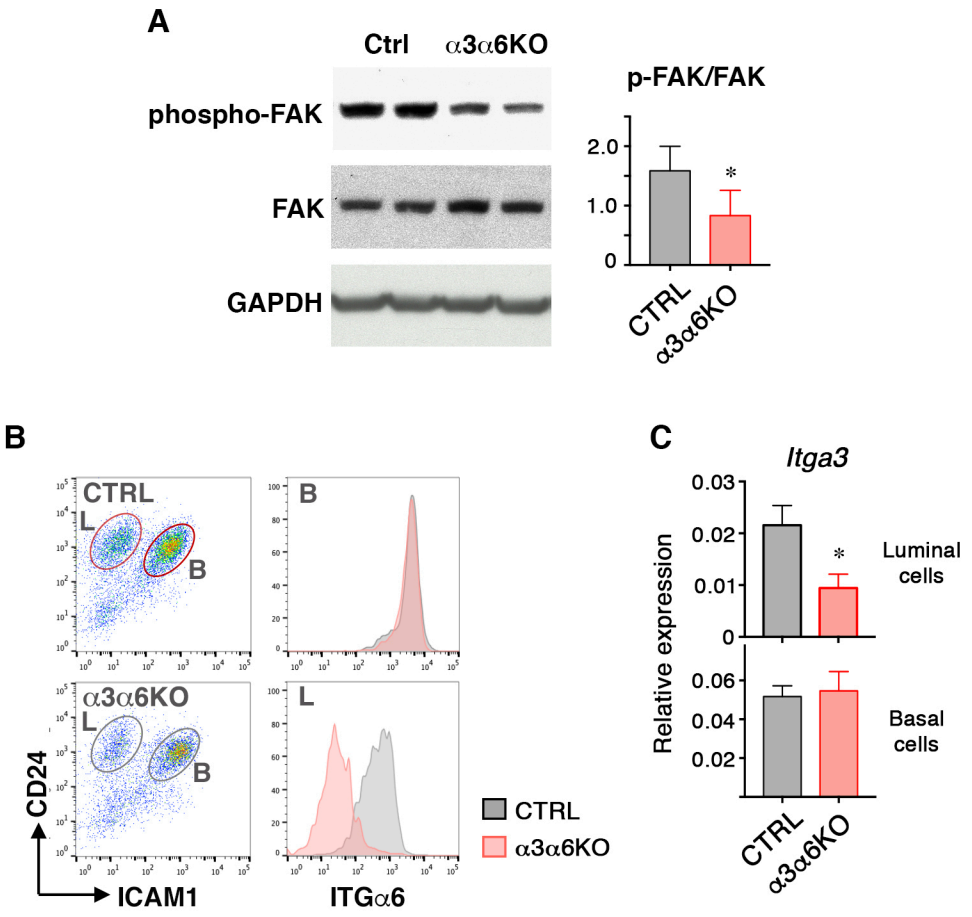

Figure S5. Analysis of integrin expression in 2-day-lactating mammary glands. Related to Figure 3.

(A) Western blotting analysis of phospho-FAK and FAK on protein extracts of 2-day-lactating mammary glands of control and α3α6KO mice. GAPDH was used as a loading control. The graph shows the means±SEM from 4 animals per genotype. p = 0.04.

(B) Left: Dot plot showing separation of basal (B) and luminal (L) cells from 2-day-lactating mammary glands on the basis of their CD24 and ICAM1 expression. Right: Basal and luminal cells were plotted for α6 integrin expression. Most of the luminal cells lack α6 integrin expression in α3α6KO glands.

(C) RT-qPCR analysis of *Itga3* expression in freshly isolated luminal and basal cells sorted from 2-day-lactating mammary glands as illustrated in B. The values were normalized to *Gapdh* and presented as means+SD from three independent experiments. p = 0.013.

Figure S6

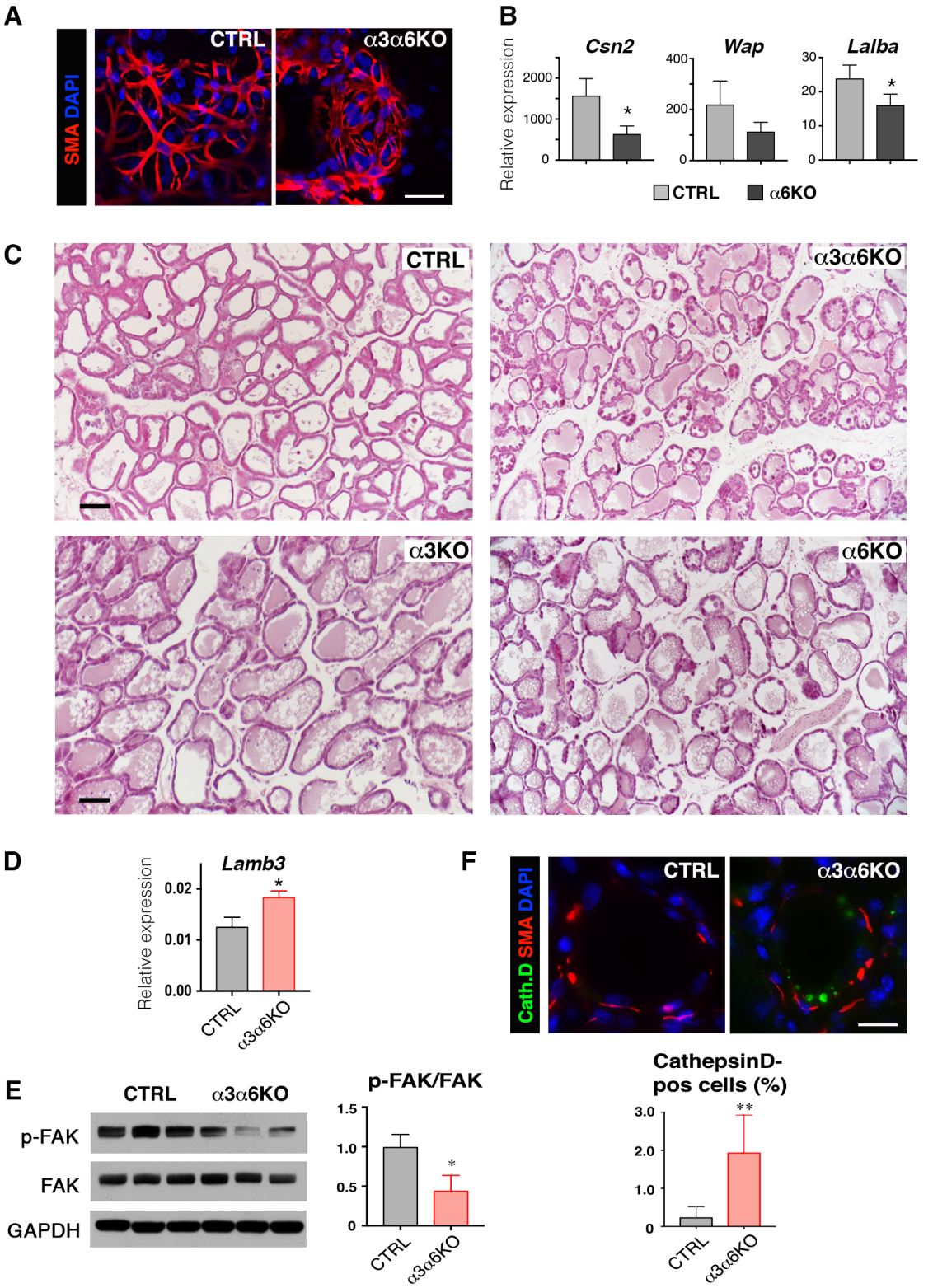

Figure S6. The deletion of LN-binding integrins from mammary luminal progenitors leads to unscheduled gland involution. Related to Figure 4**.**

(A) Immunofluorescence labeling of sections through 21-day-lactating mouse mammary glands with an antibody against α-SMA. DAPI served to visualize nuclei. Bar, 25 μm.

(B) RT-qPCR analysis of milk protein gene expression in 21-day-lactating mouse mammary glands of control and α6KO females. The graph shows means±SD; 4 females per genotype were analyzed; p = 0.015 for *Csn2*; 0.1 for *Wap*; 0.026 for *Lalba*.

(C) H&E-stained sections through 14-day-lactating mouse mammary glands. Bar, upper panels, 120 μm; lower panels, 70 μm.

(D) RT-qPCR analysis of *Lamb3* gene expression in 14-day-lactating mouse mammary glands of control and α3α6KO females. The graph shows means±SD; 3 females per genotype were analyzed; p = 0.018.

(E) Western blotting analysis of phospho-FAK and FAK on protein extracts of 2-day-lactating mammary glands of control and α3α6KO mice. β-actin was used as a loading control. The graph shows the means±SEM from 3 animals per genotype. p = 0.02.

(F) Immunofluorescence labeling of sections through 21-day-lactating mouse mammary glands with antibodies against cathepsin D and α-SMA. DAPI served to visualize nuclei. Bar, 18 μm. The graph shows the means ±SD from five microphotographs taken from two control and two α3α6KO glands. p = 0.004.

Figure S7

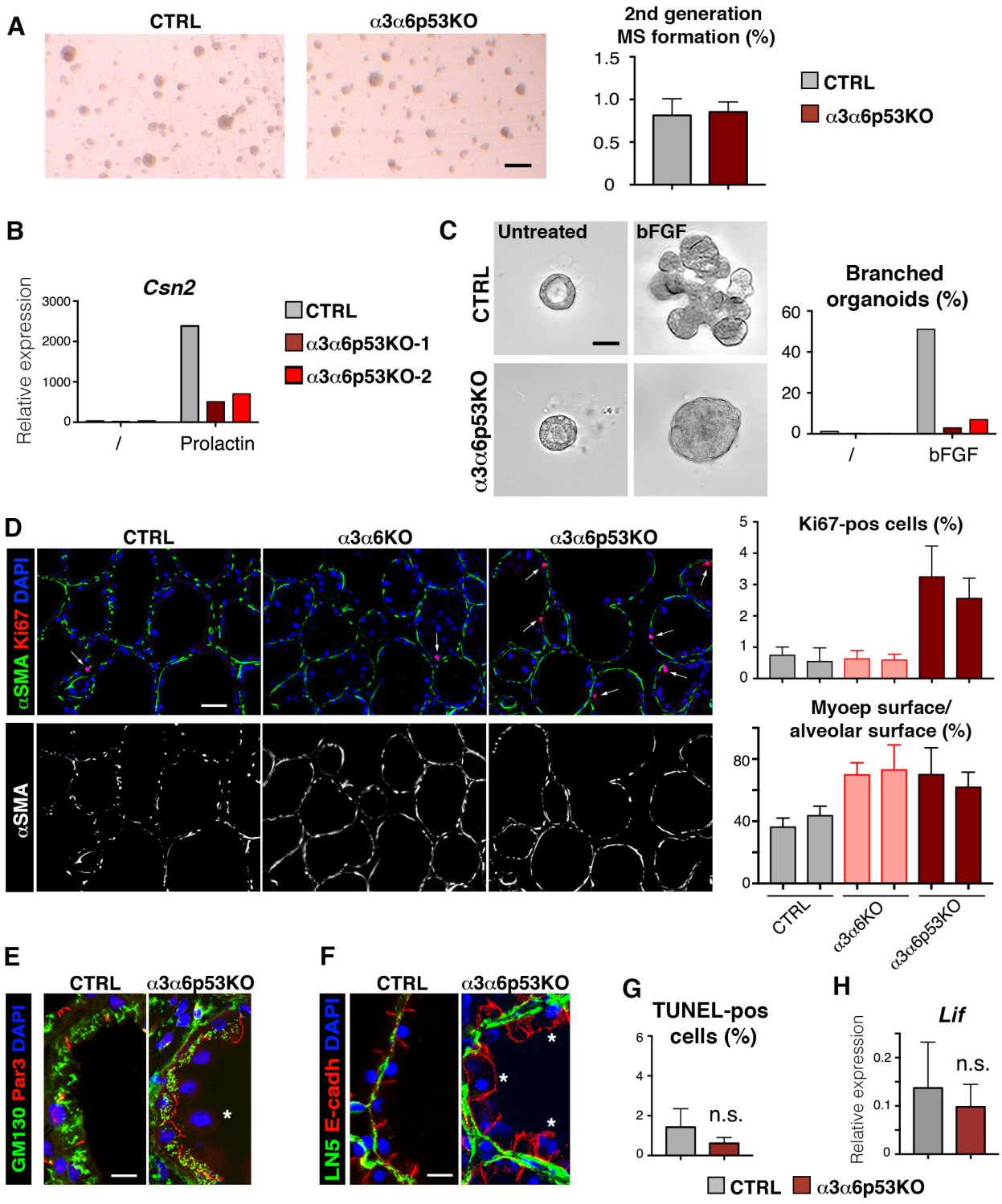

Figure S7. Genetic p53 suppression restores growth but not differentiation in mammary luminal cells depleted of LN-binding integrins. Related to Figure 5**.**

(A) Mammosphere formation by luminal ICAM1+ cells sorted from E/P stimulated mammary glands. Left: representative microphotographs (bar, 400 μm). The values shown in the graph are means±SD obtained in 3 separated wells of a representative experiment.

(B) RT-qPCR analysis of *Csn2* gene expression in mammary organoides cultured for 8-10 days in the presence or absence of prolactin. The values obtained from one control and two α3α6p53KO 15-day-pregnant glands are shown.

(C) Mammary organoids after 5 days of culture in the presence or absence of bFGF. Left, representative contrast microscopy (DIC) images. Bar, 30 μm. The graph represents the percentage of branched organoids (i.e., with 3 branches at least). The values obtained from one control and two α3α6p53KO 15-day-pregnant glands are shown.

(D) Immunofluorescence staining of control, α3α6KO and α3α6p53KO mouse mammary gland sections with antibodies against Ki67 and αSMA. The upper graph shows quantification of Ki67 positive cells. The lower graph shows the percentage of the alveolar surface covered by basal SMA+ cells. Graphs show means±SD obtained from 6 microphotographs; 2 animals per genotype were analyzed.

(E), (F) Immunofluorescence labeling of sections through 14-day-lactating mouse mammary gland with antibodies against GM130 and Par3 (F) and antibodies against the Laminin-5 and E-cadherin. DAPI served to visualize nuclei. Asterisks mark cells with aberrant Par3 and E-cadherin localization. Bar, 15 μm.

(G) TUNEL assay performed with the sections through 21-day-lactating mouse mammary glands from control and α3α6p53KO females. The graph shows means±SD; 4 females per genotype were analyzed; n.s., non significant.

(H) RT-qPCR analysis of *Lif* expression in 21-day-lactating mammary glands from control and α3α6p53KO females. The graph shows means±SD; 4 females per genotype were analyzed; n.s., non significant.

Figure S8

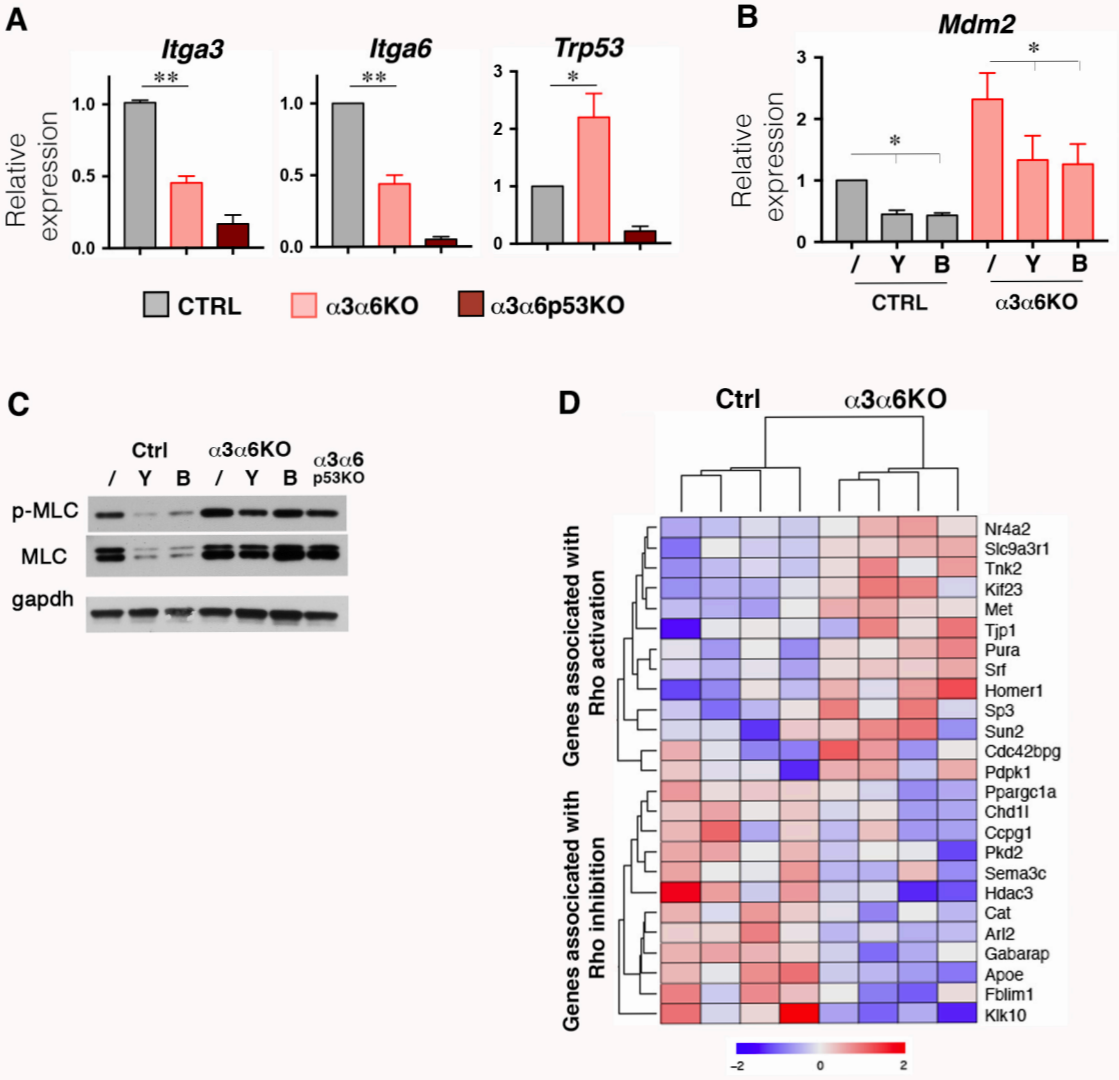

Figure S8. Activation of a Rho/MyosinII/p53 pathway downstream depletion of LN-binding integrins in mammary luminal progenitors. Related to Figure 6**.**

(A) RT-qPCR analysis of *Itga3, Itga6 and Trp53* gene expression in cells obtained from mammospheres formed by control, α3α6KO and α3α6p53KO luminal progenitor cells. The graph shows means±SD obtained in three independent experiments. p = 0.0001 for *Itga3*; 0.0004 for I*tga6*; 0.01 for *Trp53*.
(B) RT-qPCR analysis of *Mdm2* gene expression in cells obtained from mammospheres formed by luminal progenitor cells in the presence of Y27632 or Blebbistatin. The graph shows means±SD obtained in three independent experiments. For control mammospheres, p = 0.005 for Y27632-treated cells compared to non-treated cells, p = 0.02 for Blebbistatin-treated cells compared to non-treated cells. For α3α6KO mammospheres, p = 0.015 for Y27632-treated cells compared to non-treated cells, p = 0.009 for Blebbistatin-treated cells compared to non-treated cells.
(C) Western blotting analysis Phospho-MLC and MLC- protein levels in extracts of mammosphere formed by control, α3α6KO and α3α6p53KO luminal cells. GAPDH was used as a loading control. A representative experiment is shown.
(D) Heatmap based on Affymetrix analysis of freshly sorted luminal cells from 15-day-pregnant mammary glands from control and α3α6KO females.

In (A) and (B), values obtained for control cells were set as 1 in each experiment. Through the whole figure: Y, Y27632, B, Blebbistatin.

Table S1: REACTOME pathway analysis on genes differentially expressed in α3α6KO luminal cells compared to Ctrl luminal cells (p15-pregnant mice). Related to Figure 3.

Pathway Description (REACTOME)	Nb Genes in Pathway	Nb Regulated Genes (Up / Down)	P-Value (Up)	P-Value (Down)
Bmal1 : Clock, NPas2 activates circadian gene expression	21	4 (0/4)	NA	1,09E-03
Rora activates gene expression	11	3 (0/3)	NA	5,02E-03
RHO GTPases Activate Formins	111	8 (6/2)	1,15E-02	NA
SUMOylation of transcription factors	11	3 (2/1)	NA	NA
Nr1d1 (Rev-erba) represses gene expression	3	2 (0/2)	NA	2,94E-02
Transcriptional activation of mitochondrial biogenesis	14	3 (2/1)	NA	NA
Iron uptake and transport	15	3 (1/2)	NA	NA

Table S2: Antibodies used for FACs analysis of integrin expression

Antibody	Isotype	Company, Reference	Clone
ITGα1 (CD49a)	Armenian hamster IgG	Biolegend, 142603	HMα1
ITGα2 (CD49b)	Armenian hamster IgG	Biolegend, 103506	HMα2
ITGα3 (CD49c)	Goat polyclonal IgG	R&D Systems, AF2787	
ITGα5 (CD49e)	Rat IgG2a,k	Biolegend, 103805	5H10-27 (MFR5)
ITGα6 (CD49f)	Rat IgG2a,k	Biolegend, 313622	GoH3
ITGαV (CD51)	Rat IgG1,k	Biolegend, 104105	RMV-7
ITGβ1 (CD29)	Armenian hamster IgG	Biolegend, 102221	HMβ1-1
ITGβ3 (CD61)	Armenian hamster IgG	Biolegend, 104307	2C9.G2 (HMβ3-1)
ITGβ4 (CD104)	Rat IgG2a,k	Biolegend, 123609	346-11A

Table S3: Primers used for RT-qPCR analysis

Cdkn1a-s	5’ – TTCCGCACAGGAGCAAAGTG - 3’
Cdkn1a-as	5’ - CCGTGACGAAGTCAAAGTTC - 3’
Csn2-s	5’ - CCTCTGAGACTGATAGTATTT - 3’
Csn2-as	5’ - TGGATGCTGGAGTGAACTTTA - 3’
Elf5-s	5’ - CCAACGCATCCTTCTGTGAC - 3’
Elf5-as	5’ - AGGCAGGGTAGTAGTCTTCA - 3’
Gapdh-s	5’ - CCAATGTGTCCGTCGTGGATC - 3’
Gapdh -as	5’ - GTTGAAGTCGCAGGAGACAAC - 3’
Itga3-s	5’ - CACGCACATCATCACTGTTG - 3’
Itga3-as	5’ - CTGCCACCCATCATTGTTCA - 3’
Lalba-s	5’ - GACAACGGCAGCACAGAGTA - 3’
Lalba-as	5’ - GCCACAGATGTTCTCCGAC - 3’
Mdm2-s	5’ – CGCAAAACGACACTTACACTA - 3’
Mdm2-as	5’ - GCTCCTTCACAGAGAAACTC - 3’
Wap-s	5’ - TTGAGGGCACAGAGTGTATC- 3’
Wap-as	5’ - TTTGCGGGTCCTACCACAG- 3’

Other primers were purchased from SABiosciences/Qiagen.